Combined DFT and experimental studies of C–C and C–X elimination reactions promoted by a chelating phosphine–alkene ligand: the key role of *penta*-coordinate Pd^{II}

Laura Estévez,[a,b] Luke W. Tuxworth,[c,d] Jean-Marc Sotiropoulos,[a] Philip W. Dyer[c,d*] and Karinne Miqueu[a*]

[a] *Institut des Sciences Analytiques et de Physico-Chimie pour l'Environnement et les Matériaux (IPREM). Université de Pau et des Pays de l'Adour/CNRS UMR 5254. Hélioparc, 2 Avenue du Président Angot, 64053 Pau cedex 09, France. E-mail : karinne.miqueu@univ-pau.fr, Fax : + 33 (0) 559 407 862; Tel + 33 (0) 559 407 577.*
[b] *Departamento de Química Física, Universidade de Vigo, Facultade de Química Lagoas-Marcosende s/n, 36310 Vigo, Galicia, Spain.*
[c] *Centre for Sustainable Chemical Processes, Department of Chemistry, Durham University, South Road, Durham, DH1 3LE, UK. E-mail : p.w.dyer@durham.ac.uk, Fax : + 44 (0) 191 334 2150; Tel : + 44 (0) 191 384 4737.*
[d] *Department of Chemistry, Durham University, South Road, Durham, DH1 3LE, UK.*

Abstract

A combined computational and experimental study of the coordination chemistry of phosphine-alkene ligand **L1** (*N*-diphenylphosphino-7-*aza*-benzobicyclo[2.2.1]hept-2-ene) with Pd^0 and Pd^{II} is presented. Experimentally it is established that ligand **L1** promotes direct alkyl-alkyl and indirect alkyl-halide reductive elimination from Pd^{II} species, affording palladium(0) complex [Pd(κ^2-P,C-**L1**)$_2$] (**2**) in each case. The effectiveness of **L1** in promoting these reactions is attributed to the initial formation of a *penta*-coordinate intermediate [PdMe(X)(κ^1-P-**L1**)(κ^2-P,C-**L1**)] (X = Me, Cl) coupled with the ease with which it transforms to **2**. From computation, a lower activation barrier for C(sp^3)–C(sp^3) coupling and subsequent elimination has been computed for a stepwise associative pathway involving initial formation of [PdMe$_2$(κ^1-P-**L1**)(κ^2-P,C-**L1**)], compared to that computed for direct elimination from its parent, *cis*-[PdMe$_2$(κ^2-P,C-**L1**)]. Moreover, the C(sp^3)–C(sp^3) coupling reaction has been found to be primarily under thermodynamic control. It has also been demonstrated computationally that the methyl group of *penta*-coordinate [PdCl(Me)(κ^1-P-**L1**)(κ^2-P,C-**L1**)] is susceptible to nucleophilic attack by the phosphorus lone pair of a further equivalent of ligand **L1**, which proceeds through an S_N2-like transition state. This initiates an unusual, indirect intermolecular reductive elimination process, resulting in formation of equimolar quantities of the methyl phosphonium chloride salt of **L1** and complex **2**, in agreement with experimental observations. In contrast to the C(sp^3)–C(sp^3) coupling, computation shows that this indirect C(sp^3)–Cl reductive elimination process is essentially under kinetic control.

Introduction

Today, palladium-mediated cross-coupling reactions for the formation of C–C and C–heteroatom bonds are a cornerstone of organic synthesis. The versatility of these transformations has led to the development of a host of different catalytic systems based on phosphine complexes of palladium(0) and palladium(II), in particular.[1-3] Although it is well established that these types of reaction involve three important fundamental steps, namely oxidative addition, transmetallation and reductive elimination, considerable mechanistic work remains in order to fully understand and hence optimise catalytic performance and selectivity.

Of particular importance is the efficacy of the reductive elimination step, which is essential for the delivery of the final product (Scheme 1). Here, experiment has shown that the rate of reductive elimination is intimately linked not only to the nature of the coupling partners (R), but also to the ancillary ligands (L), in particular to their steric and electronic characteristics.[4-6] Complexes that possess sterically demanding ligands have achieved particular success. Not only is their bulk believed to enhance the rate of reductive elimination as a result of the relief of steric congestion about the palladium centre upon product formation, but bulky ligands also promote the formation of low coordinate, unsaturated Pd^0 species that show enhanced reactivity in Pd-catalyzed cross-coupling reactions, particularly in the substrate oxidative addition step.[7] Similarly, systems incorporating weakly *trans* influencing, poorly-donating/electron-accepting phosphine ligands have attracted considerable interest since they reduce the electron density at the metal centre, which facilitates reductive elimination from the square planar palladium intermediates.[8]

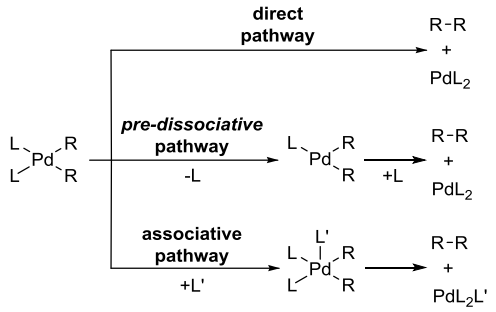

Scheme 1 Potential mechanisms for reductive elimination from *tetra*-coordinate palladium(II) complexes.

In order to broaden understanding of this key palladium-mediated cross-coupling reaction step several theoretical studies have been undertaken.[9] Early work by Hoffmann[10] and Goddard[11] probed the role of the essential ancillary phosphine ligands in these systems, something extended more recently by Morokuma and co-workers, who investigated the effect of various phosphines (PH_3, PMe_3, PPh_3, P{*c*-hexyl}$_3$) using ONIOM computational methods.[12] These studies explored the two most common reductive elimination pathways, one involving *tetra*-coordinate complexes and one T-shaped *tri*-coordinate species, the latter formed by ligand pre-dissociation (Scheme 1). Activation barriers computed for these two reaction paths lie in the range 18 to 26 kcal mol^{-1}, with those for processes involving *tri*-coordinate T-shaped species being lower than those for the *tetra*-coordinate complexes. Which of these two different mechanistic manifolds that is accessed is shown to be controlled primarily by the nature of the phosphine ligands employed, with steric effects in particular controlling the structure of the square planar Pd^{II} complexes in accord with observations made experimentally (*vide supra*). The electronic character of the phosphine ligands is found to influence strongly the structure and energies of the various reaction transition states. The impact of these effects was qualified further in a related theoretical study by Ariafard and

Yates, who showed that reductive elimination is more favourable when sterically-demanding, weakly basic, π-accepting ligands are employed. For example, the rate of formation of ethane from $[PdMe_2(PR_3)_2]$ *via* reductive elimination has been found to be faster on using PCl_3 compared with use of PMe_3, something attributed to the destabilisation of the initial dimethyl phosphine complex.[13] An analogous computational study by Maseras and co-workers explored R–R (R = Me, Ph, vinyl) coupling reactions from *cis*-$[PdR_2(L)(PMe_3)]$ complexes *via* reductive elimination, where L is either acetonitrile, ethylene or maleic anhydride.[14] Here, the steric demands and the electronic character of the organyl group R, the phosphine and the mode of coordination of the co-ligand L all strongly influence the coupling mechanism. In particular, the influence of the coupling partners R was highlighted, with reductive elimination involving $C(sp^2)$–$C(sp^2)$ bond formation being computed to be more facile than that involving $C(sp^3)$–$C(sp^3)$ coupling. Morokuma and colleagues have further explored the impact of the hydrocarbyl groups on reductive elimination by studying reactions of square planar *cis*-$[PdR(R')(PH_3)_2]$ palladium complexes (R, R' = methyl, vinyl, phenyl, alkynyl) computationally.[15] Again, the nature of the organyl species undergoing coupling has a significant impact on the magnitude of the activation barrier for reductive elimination, which increases in the order $C(sp^2)<C(sp)<C(sp^3)$.

In contrast to the wealth of theoretical reports exploring the formation of C–C bonds *via* reductive elimination, comparatively few computational studies of the analogous processes of C–heteroatom[16] and C–halogen[17] bond formation have been reported, despite their broad synthetic importance in organic chemistry.[18] This is particularly surprising since a host of experimental studies have been described in these areas.[2,5,19] Once again, as is the case for palladium-mediated C–C bond formation, analogous processes for the formation of C–heteroatom bonds are also subject to significant effects imposed by the steric and electronic characteristics of both the coupling partners and ancillary ligands.

An important strategy for enhancing the rates of reductive elimination during palladium-mediated C–E bond-forming reactions (E= C, halide, heteroatom) is the use of chelating ligands. In complexes such as *cis*-[PdR(X)(κ^2-P,P-diphosphine)] the diphosphine's bite angle has a significant impact on the R–Pd–X bond angle and hence on the rate of R-X coupling.[20]To further understand these effects, the role of bidentate diphosphine ligands in reductive elimination from Pd^{II} has been probed computationally and shows that as the bite angle for chelating diphosphines $H_2P(CH_2)_nPH_2$ (n = 1-4) is increased, an acceleration in the rate of reductive elimination occurs.[16b] This results from destabilisation of reactant palladium complex and stabilisation of the associated transition state.

The wealth of information available about palladium-mediated cross-coupling reactions from both theoretical and experimental studies, has led to the development of an important class of unsymmetrical heteroditopic ligands. These systems combine the geometric and steric constraints imposed by *cis*-bidentate coordination with the electronic impact of a σ-donating phosphine moiety coupled with a π-accepting alkene unit, to promote very effectively reductive elimination from Pd^{II} systems.[21] In related studies, we have recently reported the use of the new chelating phosphine-alkene ligand **L1** (Scheme 2).[22] This metal scaffold was developed in order to exploit the inherent electronic asymmetry conferred by the combination of a weakly basic, amido-substituted $PPh_2(NR_2)$ σ-donor moiety with a π-accepting alkene unit in a strained bicyclic 7-*aza*-norbornene motif, with a view to maximising Pd-to-alkene π-back-donation through relief of ring strain. Indeed, not only does ligand **L1** enhance the rate of alkyl-alkyl coupling reactions, but it also enables an unusual, indirect alkyl-chloride reductive elimination process, which results in the generation of the methyl phosphonium chloride salt of **L1** together with the extremely stable palladium(0) complex [Pd(κ^2-P,C-**L1**)$_2$].

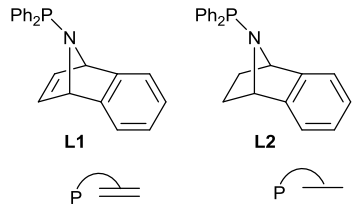

Scheme 2 *N*-Diphenylphosphino-7-*aza*-benzobicyclo[2.2.1]hept-2-ene ligand (**L1**) and the corresponding phosphine-alkane derivative (**L2**).

In order to gain greater insight into the influence of this new family of electronically unsymmetrical phosphine-alkene ligands **L1** on the experimentally observed C–C coupling reactions and to investigate the course of the unusual C–Cl elimination reaction, we have performed DFT calculations on a range of $PdMe_2$(**L1**) and PdCl(Me)(**L1**) species, as well as related studies involving the phosphine-only ligand, **L2** (Scheme 2). The results of these studies are presented here.

Results and discussion

Experimental data and computational studies involving $PdMe_2$ fragments

Experimental results

Treating a toluene solution of [$PdMe_2$(tmeda)] (tmeda = *N*,*N*,*N'*,*N'*-tetramethylethane-1,2-diamine) with one equivalent of the phosphine-alkene ligand **L1**, affords the complex *cis*-[$PdMe_2$(κ^2-P,C-**L1**)] (**1**), with conversion being complete within ~5 minutes (Scheme 3).[22] At room temperature (r.t.) a toluene solution of complex **1** slowly undergoes spontaneous reductive elimination to afford the very stable palladium(0) *bis*(phosphine-alkene) complex

[Pd(κ^2-P,C-**L1**)$_2$] (**2**) and ethane, together with elemental palladium. Complete consumption of complex **1** is achieved after 120 h at room temperature.

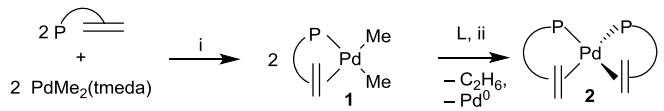

Scheme 3 (i) toluene, r.t., ~5 mins, >99% ; (ii) general conditions, toluene, r.t., >99% conversion: L = nothing, 120 h; L = **L1**, 5 h; L = PPh_3 (5 mol%), 7 h; L = propene (5 mol%), 30 h.

Notably, on treating [$PdMe_2$(tmeda)] with two equivalents of phosphine-alkene ligand **L1**, the rate of reductive elimination is considerably increased, with complete conversion to complex **2** taking just 5 h at r.t. Furthermore, comparable enhancements in the rate of reductive elimination are also achieved through addition of either 5 mol% Ph_3P or propene to complex **1**, with conversions being complete in 7 and 30 h, respectively at r.t. (Scheme 3).[22] It was proposed that these observations could be accounted for by the presence of the additional L-donor ligands (L = **L1**, Ph_3P, propene) that opens a new reaction pathway for reductive elimination, which involves the formation of a *penta*-coordinate complex such as [$PdMe_2$(L)(κ^2-P,C-**L1**)].[22] This is consistent with prior reports of rate enhancements in palladium-mediated reductive elimination as a result of increased coordination number prior to elimination.[23] Moreover, it has been reported that the specific addition of olefinic *co*-ligands can significantly augment the rate of reductive elimination from palladium as a result of their acceptor character, which reduces the electron density at the metal centre to which they are bound.[14] Thus, it was important to probe the potential role of simply the olefinic moiety of **L1** in promoting reductive elimination rather than the phosphine-alkene ligand as a whole. Consequently, the coordination chemistry of the related phosphine-alkane derivative

L2 was probed experimentally, but was found to confer completely different reactivity. While reaction of two equivalents of ligand **L1** with [$PdMe_2$(tmeda)] promotes rapid reductive elimination and the formation of equimolar quantities of complex **2** and ethane, the analogous reaction with phosphine-alkane ligand **L2** affords initially *cis*-[$PdMe_2(\kappa^1$-P-**L2**$)_2$] (Scheme 4). This complex then isomerises cleanly to the *trans*-diphosphine complex within 24 h at r.t; no further reaction of *trans*-[$PdMe_2(\kappa^1$-P-**L2**$)_2$] is observed even in the presence of excess **L2** at 60 ºC.[22] Although these observations suggest that κ^2-P,C chelation is vital in retaining the *cis*-dialkyl geometry for reductive elimination, it remains unclear whether the coordination of the olefinic moiety of **L1** also plays an electronic role in promoting reductive elimination. Thus, it was of interest to probe both the coordination chemistry of ligands **L1** and **L2** and the subsequent reactivity of their palladium complexes computationally.

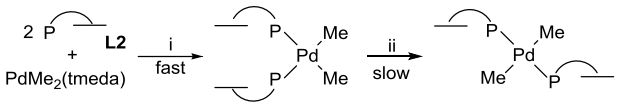

Scheme 4 (i) toluene, r.t., ~5 mins, >99% ; (ii) toluene, r.t., ~24 h, >99% conversion.

Computational studies: reductive elimination reaction profiles involving $PdMe_2$ fragments

DFT calculations were performed at the B97D/SDD+f(Pd), 6-31G** (other atoms) level of theory (see computational details) to evaluate the formation of ethane *via* a C–C coupling and reductive elimination process from the chelated phosphine-alkene palladium complex *cis*-[$PdMe_2(\kappa^2$-P,C-**L1**$)$] (**1**). A focus of this paper is an exploration of the effect of varying the Pd:**L1** ratio, 1:1 and 1:2, on the reductive elimination reaction profile.

Furthermore, the roles of additional PPh_3 and propene in promoting reductive elimination from the dimethyl complex **1** have also been probed. Each stage of the various pathways for reductive elimination from complex **1** (Scheme 5) has been probed computationally and the more relevant Gibbs free energy values are shown in Fig. 1 (additional data are listed in Table S1 in the Electronic Supplementary Information); the structures of the reactants and the transition states are depicted in Fig. 2.

Structural analysis of *cis*-[$PdMe_2(\kappa^2$-P,C-L1)] (1)

As a starting point for the computational study and in order to verify the computational methods employed, the structure of [$PdMe_2(\kappa^2$-P,C-**L1**)] (**1**) was computed and the resulting metric parameters compared with those determined experimentally by X-ray diffraction, an analysis that revealed a good correlation between theory and experiment.[24] The square planar geometry around palladium is reproduced, together with the bidentate (κ^2-P,C) phosphine-alkene coordination of **L1** in which the olefinic moiety of the 7-*aza*-benzobicyclo[2.2.1]hept-2-ene moiety is bound in an η^2 fashion and orientated perpendicular to the metal square plane, as would be expected for a d^8 metal centre as a result of geometric constraints.[22] Computational analysis shows the olefinic moiety of **L1** to be bound in a symmetrical fashion with identical Pd–C_{olefin} bond distances of 2.28 Å (Fig. 2), something that differs slightly from the unsymmetrical coordination found in the X-ray structure with Pd–C_{olefin} distances of 2.238(2) and 2.266(2) Å. The C=C bond distance for the palladium-bound olefinic moiety is computed to be 1.39 Å (*cf.* X-ray: 1.359(3) Å), which is slightly longer compared to that computed for the free ligand **L1**, 1.34 Å, as expected for κ^2-P-C chelate binding of **L**.[22] Topological analysis of the electron density associated with complex **1**, using Atoms in Molecules (AIM) theory (see Computational details), further confirms the chelate coordination of **L1**, with a ring critical point being found between the three atoms

Pd,$C1_{olefin}$,$C1'_{olefin}$ (ρ(r)= 0.067 au). Natural Bond Orbital (NBO) analysis of complex **1** highlights a strong stabilizing interaction (ΔE_2) between the $\pi_{C=C}$ orbital of the alkene and the Pd centre of 53.5 kcal mol^{-1} (ligand→metal donation) and a weaker Pd/$\pi^*_{C=C}$ orbital interaction of 24 kcal mol^{-1} (metal→ligand back-donation). In contrast to the expectation that the olefinic component of **L1** would be subject to significant Pd→$\pi^*_{C=C}$ back-donation in order to relieve ring strain in the *aza*-norbornene skeleton,[22] these computationally-derived data are consistent with only moderate back-donation. However, this bonding situation is in good agreement with that computed (at the B3LYP/dgdzvp level of theory) for a palladium analogue of Zeise's salt $[PdR_3(\eta^2\text{-}C_2H_4)]^-$ (olefin orientated perpendicular to the square plane), where values for back-donation are in the range, ΔE_2 = 17.2 kcal mol^{-1} (R = C_6F_5) and ΔE_2 = 28.3 kcal mol^{-1} (R = Cl), consistent with limited Pd→olefin back-donation as would be anticipated for weakly π-basic d^8 Pd centre.[25]

As is determined experimentally by X-ray diffraction, the two Pd–Me bond distances of complex **1** are computed to be essentially equivalent 2.097 and 2.098 Å (*cf.* X-ray: 2.068(3) and 2.074(3) Å), despite being located *trans* to the phosphine and *trans* to the olefin moieties, respectively. The computed Pd–P bond distance of 2.323 Å is in moderate agreement with that determined by X-ray diffraction (2.2876(6) Å), with the P–N bond distance being computed to be slightly longer than that for the free ligand (from 1.74 Å in free **L1** to 1.76 Å in **1**), and in good agreement with the distance determined 1.732(2) Å in the complex. This slight P–N bond lengthening results presumably from metal→phosphorus back-donation into a P-R σ* orbital.[26]

Reactivity of *cis*-[$PdMe_2(\kappa^2$-P,C-L1)] (1)

It has been shown experimentally that the presence of the potentially coordinating olefin moiety of phosphine-alkene ligand **L1** is crucial in accessing a reductive elimination pathway from its $PdMe_2$ complexes. Indeed, the product from the reaction of [$PdMe_2$(tmeda)] with the comparable monodentate phosphine-alkane **L2** is subject to facile *cis*-to-*trans*-isomerisation, which prevents reductive elimination. Thus, in order to gain greater insight into the precise role of the κ^2-P-C chelation of **L1** upon the palladium centre a series of computational investigations have been undertaken.

Two reaction pathways may be envisaged to account for the observed reductive elimination from complex **1**, namely a *pre-dissociative* route *via* a *tri*-coordinate complex and a direct elimination from the square planar parent complex (Scheme 5, *pre-dissociative* route and Path A). As a starting point for the investigation of the *pre-dissociative* pathway, the structure of the model *tri*-coordinate T-shaped complex *cis*-[$PdMe_2(\kappa^1$-P-**L1**)] (**1'**) was computed (Fig. 2).

Analysis of the geometry of complex **1'** reveals a short H···Pd distance of 2.92 Å with a Pd–H–C bond angle of 144.5°, values that are consistent with an electrostatic anagostic interaction of one of the Csp^3–H bonds of the *aza*-norbornene framework and the metal centre (M···H distances and M–H–C bond angles for anagostic bonds fall in the ranges 2.3-2.9 Å and 110-170°, respectively).[27] The presence of the weak H···Pd anagostic interaction in **1'** is further supported by AIM analysis (Fig. S1 in ESI), confirming a bond path connecting the H atom and the Pd metal centre.[28] Furthermore, the properties at the bond critical point (BCP) along this bond path, $\rho(\mathbf{r})$ = 0.010 au and $\nabla^2\rho(\mathbf{r})$ = +0.031 au, confirm the anagostic nature of this interaction (for agostic interactions $\rho(\mathbf{r})$ values are usually found to be higher ~0.02 au).[27,29]

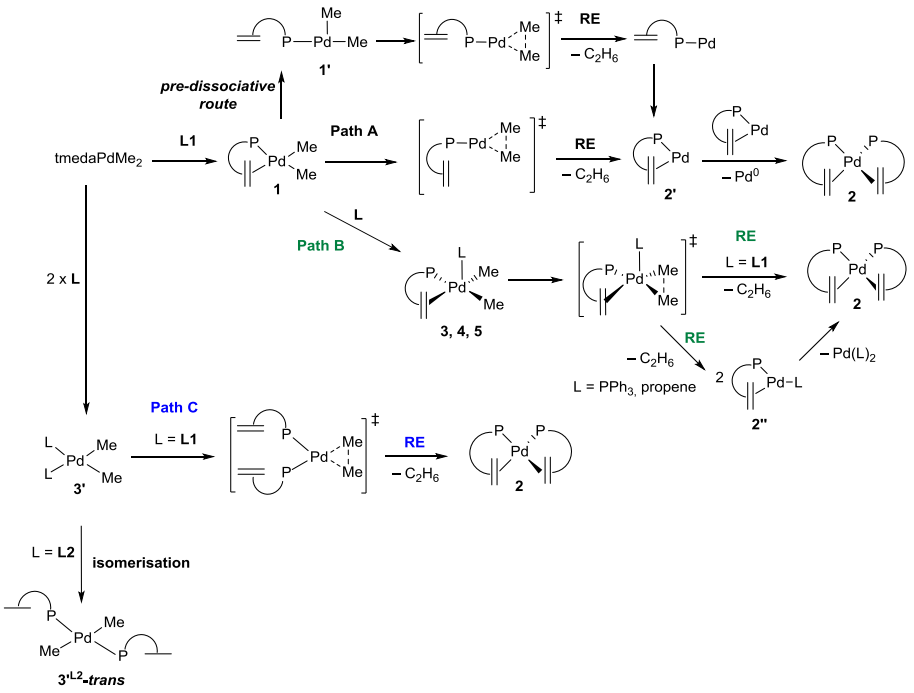

Scheme 5 Reductive elimination (RE) pathways from *cis*-[$PdMe_2(\kappa^2$-P,C-**L1**)] (**1**) (Path A), from the *penta*-coordinate [$PdMe_2(\kappa^1$-P-**L**)(κ^2-P,C-**L1**)] complexes (Path B) with L being **L1** (**3**), PPh_3 (**4**), propene (**5**), respectively, and from *tetra*-coordinate *cis*-[$PdMe_2(\kappa^1$-P-**L1**$)_2$] (**3'**) (Path C).

A computational analysis of the model *tri*-coordinate T-shaped complex *cis*-[$PdMe_2(\kappa^1$-P-**L1**)] (**1'**) reveals that it is 10.6 kcal mol^{-1} less stable than complex **1**, something consistent with a strong olefin-Pd interaction in **1**.[30] The activation barrier for the $H_3C–CH_3$ coupling reaction *via* reductive elimination from the *tri*-coordinate complex **1'** is 15.8 kcal mol^{-1}, which lies in the range of energies computed from similar [$PdMe_2(PR_3)$] complexes.[12,14]

In a similar fashion, the alternative *direct pathway* for C–C coupling from the *tetra*-coordinate square planar dimethyl complex **1** was probed computationally (Scheme 5, Path A). These studies reveal that, as expected, the mechanism is concerted,[4,31] with an activation barrier of 28.1 kcal mol^{-1} (Fig. 1, Path A). At the transition state, there is a decrease in both the incipient C···C bond distance (from 2.867 to 2.030 Å) and the C_{Me}-Pd-C_{Me} bond angle

(from 86.2° to 55.5º), accompanied by an increase in the Pd–C_{Me} bond distances from 2.097 and 2.098 Å in **1** to, respectively, 2.129 and 2.226 Å in the $\mathbf{TS_{1\rightarrow 2}}$ (Fig. 2). A decrease in the P–Pd bond distance from 2.32 Å to 2.25 Å is found, which is consistent with the decrease in electron density at palladium caused by the on-set of the reduction process being compensated by an increase in donation from phosphorus to palladium. However, this change in the Pd–P interaction is accompanied by dissociation of the olefinic unit of **L1** from the palladium centre in the $\mathbf{TS_{1\rightarrow 2}}$ with the Pd···C_{olefin} distance becoming 3.6 Å (*cf.* 2.28 Å in **1**), something paralleled by the expected reduction in C=C bond distance to 1.35 Å, comparable to that computed for the non-coordinated, free olefin (1.34 Å). This olefin dissociation is confirmed *via* AIM analysis of the $\mathbf{TS_{1\rightarrow 2}}$, structure which indicates that there is no olefin–Pd bonding interaction (see ESI, Fig. S1). Together, these structural distortions mean that the Pd centre of $\mathbf{TS_{1\rightarrow 2}}$ is essentially *tri*-coordinate, exhibiting a distorted Y-shaped structure similar to that found for *cis*-[$PdMe_2$(κ^1-P-**L1**)] (**1'**) (P–Pd: 2.258 Å; PdMe: 2.125 Å, 2.201Å; MePdMe: 56.7° in **1'**).

Overall, it is found that the two transition states $\mathbf{TS_{1\rightarrow 2}}$ and $\mathbf{TS_{1'\rightarrow 2}}$ associated with reductive elimination *via* the direct pathway from complex **1** or through the *pre-dissociative* mechanism involving complex **1'** are very similar (comparable geometrical parameters and an energy difference of only 1.6 kcal mol^{-1}, Fig. 1). Thus the difference in the calculated activation barriers (15.8 *vs* 28.1 kcal mol^{-1}) for the two paths can largely be attributed to the stabilization of complex **1** by the κ^2-P,C chelation of ligand **L1**, as previously reported in the literature for related bidentate ligand systems.[4]

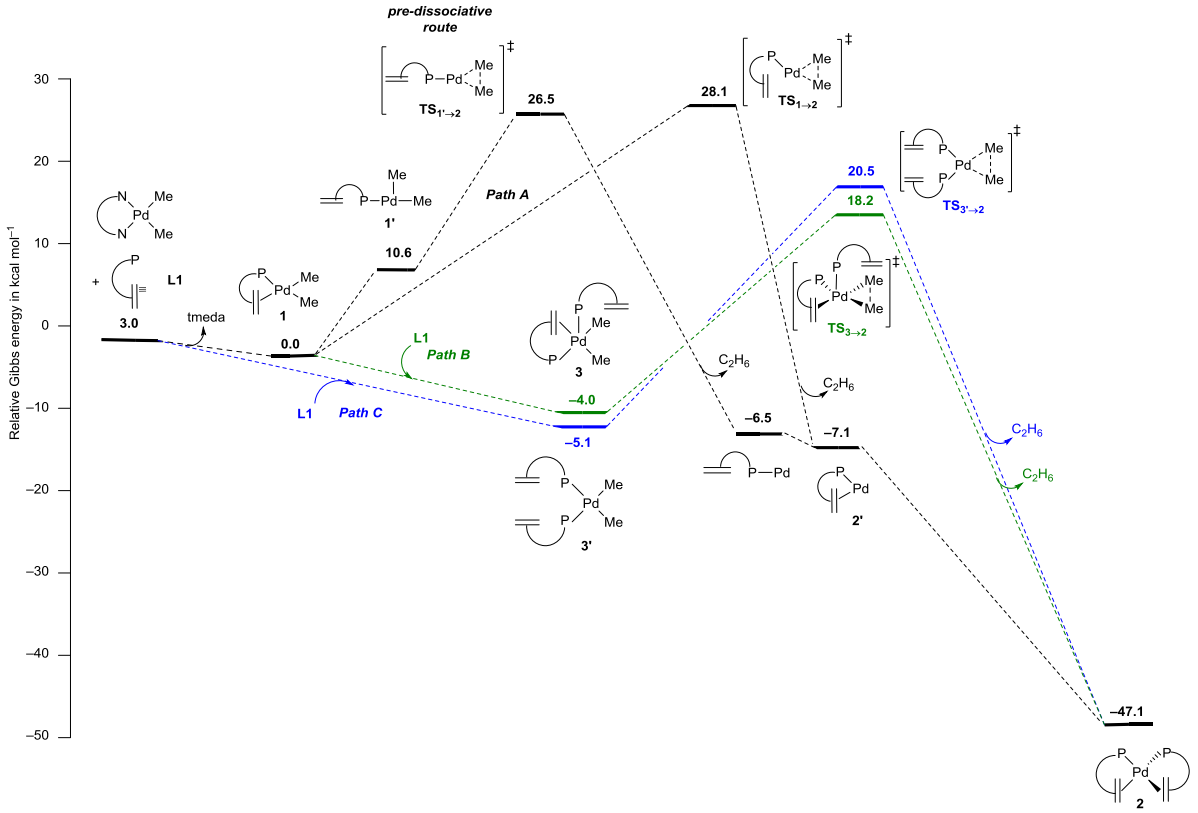

Fig. 1 Gibbs free energy profile (ΔG values in kcal mol^{-1}) for reductive elimination involving i) Path A : the starting complex *cis*-[$PdMe_2(\kappa^2$-P,C-**L1**)] (**1**) (direct or *pre-dissociative* mechanism); ii) Path B : the *penta*-coordinate intermediate [$PdMe_2(\kappa^1$-P –**L1**)(κ^2-P,C-**L1**)] (**3**); and iii) Path C : the *tetra*-coordinate complex *cis*-[$PdMe_2(\kappa^1$-P-**L1**)$_2$] (**3'**).

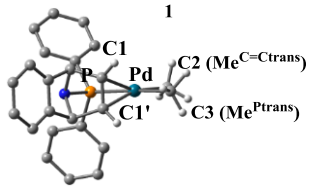

P-Pd: 2.32; Pd-C(Me): 2.10;
C1/C1'-Pd: 2.28; C1=C1': 1.39;
MePdMe: 86.2

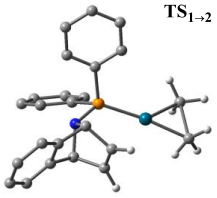

P-Pd: 2.25; Pd-C2: 2.23;
Pd-C3: 2.13; C1=C1': 1.35.
Me-Me: 2.03; MePdMe: 55.2

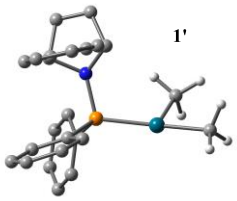

P-Pd: 2.33; Pd-C2:2.06; Pd-C3:2.07
C1=C1':1.34; MePdMe:86.6

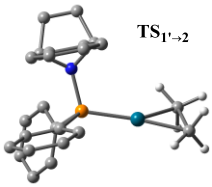

P-Pd: 2.26; Pd-C2:2.20; Pd-C3:2.13
C1=C1':1.34; MePdMe:56.7

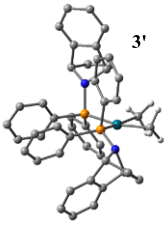

P-Pd: 2.36; P-Pd: 2.31; Pd-Me: 2.13;
PPdP: 100.6; MePdMe: 80.2

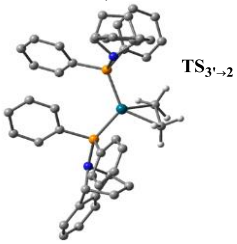

P-Pd: 2.32; Pd-Me: 2.24;
Me-Me: 2.05; PPdP: 119.4; MePdMe: 54.3

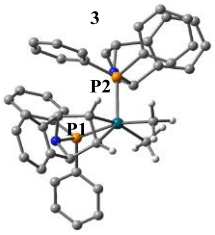

P2-Pd: 2.45; Pd-C2: 2.16; Pd-C3: 2.12;
C1-Pd: 2.21; C1'-Pd: 2.26; C1=C1': 1.42;
P1-Pd: 2.35; PPdP: 99.2; MePdMe: 83.0

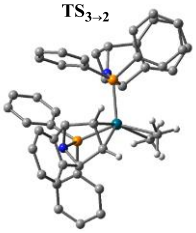

P2-Pd: 2.33; Pd-Me: 2.33; C1-Pd: 2.23;
C1'-Pd: 2.30; C1=C1': 1.41; P1-Pd: 2.47;
Me-Me: 2.02; PPdP: 100.8; MePdMe: 51.6

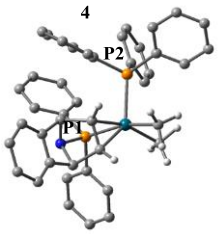

P2-Pd: 2.44; Pd-C2: 2.16; Pd-C3: 2.12;
C1-Pd: 2.21; C1'-Pd: 2.25; C1=C1': 1.42;
P1-Pd: 2.36; PPdP: 99.2; MePdMe: 82.1

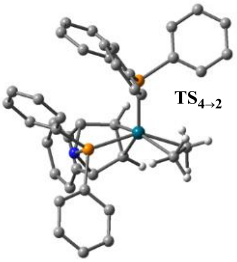

P2-Pd: 2.353; Pd-Me: 2.32; C1-Pd: 2.23;
C1'-Pd: 2.27; C1=C1':1.41; P1-Pd: 2.48
Me-Me: 2.01; PPdP: 100.0; MePdMe: 51.6

Fig. 2 Optimized geometries of the starting complex *cis*-[$PdMe_2(\kappa^2$-P,C-**L1**)] (**1**) and the transition state $\mathbf{TS_{1\rightarrow 2}}$ for the reductive elimination process forming ethane, the *pre-dissociative* mechanism from *cis*-[$PdMe_2(\kappa^1$-P-**L1**)] (**1'**) and the transition state $\mathbf{TS_{1'\rightarrow 2}}$ together with those of the *tetra*-coordinate complex *cis*-[$PdMe_2(\kappa^1$-P-**L1**)$_2$] (**3'**), *penta*-coordinate species [$PdMe_2(\kappa^1$-P-L)(κ^2-P,C-**L1**)] (L = **L1** (**3**), L = PPh_3 (**4**)) and corresponding transition states $\mathbf{TS_{3'\rightarrow 2}}$, $\mathbf{TS_{3\rightarrow 2}}$, $\mathbf{TS_{4\rightarrow 2}}$. Selected bond distances (in Å) and bond angles (in degrees).

After reductive elimination is complete (Scheme 5, path A), ligand **L1** remains bound in a κ^2-P,C fashion in the resulting palladium(0) complex [Pd(κ^2-P,C-**L1**)] (**2'**). Consistent with the electron-rich nature of the palladium centre of **2'**, the olefin moiety of bound **L1** is subject to Pd→π^*(C=C) back-donation (NBO analysis ΔE_2 : 33.6 kcal mol^{-1} in **2'** *versus* 24.1 kcal mol^{-1} in **1**). This is reflected in a slight shortening of the Pd–C_{olefin} bond distances (from 2.28 Å in **1** to 2.24 Å in **2'**) and a lengthening of the olefinic C–C bond {C–C: 1.40 Å (**2'**); 1.39 Å (**1**); 1.34 Å (**L1**)}.

The low coordination number of **2'**, coupled with the electron-rich nature of the palladium centre, renders this complex unstable and only weakly thermodynamically favoured (–7.1 kcal mol^{-1}). Consequently, **2'** is likely to undergo ligand dissociation leading to the formation of elemental Pd, as observed experimentally and free ligand **L1**. The latter could then react with another molecule of **2'** affording the stable homoleptic *bis*(phosphine-alkene) complex [Pd(κ^2-P,C-**L1**)$_2$] (**2**), consistent with experimental results. This reaction course is supported by a strongly exergonic Gibbs energy change upon coordination of ligand **L1** to **2'** (ΔG = –40.0 kcal mol^{-1}). As anticipated, this coordination of a second equivalent of **L1** leads to a further elongation of both the coordinated olefin C–C bonds and the Pd–P distances to 1.42 and 2.33 Å, respectively, and a slight shortening of the Pd–C_{olefin} bond distances (2.23/2.21 Å), in the final product [Pd(κ^2-P,C-**L1**)$_2$] (**2**). These computed structural parameters for complex **2** are comparable to those determined experimentally by X-ray diffraction (C=C: 1.401(2) and 1.406(2) Å; Pd–P: 2.3440(4), (2) 2.3341(4)).[22]

For Path A (Fig. 1), we have shown above that the Gibbs energy barrier to reaching **TS1→2** is 28.1 kcal mol^{-1}, a value that lies within the range of activation energies reported previously for reductive elimination involving C(sp^3)–C(sp^3) coupling reactions.[14,15]

Furthermore, our calculations predict that reductive elimination from **1**, leading first to the unstable low-coordinate species **2'**, is weakly exergonic ($\Delta G_{1\rightarrow 2'}$ = –7.1 kcal mol^{-1}). This contrasts with a previous report describing reductive elimination from [$PdR_2(PR'_3)_2$] (R = methyl, phenyl, vinyl, ethynyl; R' = H, Me) and [$PdR_2(L)(PMe_3)$] (R = Me, vinyl, phenyl; L = malonate, ethylene, acetonitrile) systems,[14,15] with computed $\Delta G_{\text{reaction}}$ values here lying between –30 and –50 kcal mol^{-1} (*i.e.* reactions that are significantly exergonic).

Together these data indicate that the slow reaction observed on treating [$PdMe_2$(tmeda)] with one equivalent of **L1** is not only a result of kinetic control (activation barrier of 28.1 kcal mol^{-1}), but also a consequence of thermodynamic constraints imposed by the weakly exergonic reaction leading to **2'**, which then evolves to the *bis*(**L1**) complex **2** after release of elemental palladium.

Addition of a second equivalent of L1 to [$PdMe_2(\kappa^2$-P,C-L1)] (1)

As mentioned above, it has been shown experimentally that the rate of formation of ethane from [$PdMe_2(\kappa^2$-P,C-**L1**)] (**1**), and associated formation of the palladium(0) complex **2** (120 h), is enhanced considerably in the presence of a second equivalent of **L1** (reaction complete within 5 h). Probing the reaction of [$PdMe_2$(tmeda)] with two equivalents of ligand **L1** computationally shows that reductive elimination is exergonic, with the computed value of $\Delta G_{1\rightarrow 2}$ being –47.1 kcal mol^{-1} (Fig. 1), which lies in the range found typically for $H_3C–CH_3$ coupling (Scheme 5).[14,15] Note that for Pd:**L1** ratio of 1:2, no elemental Pd is released. We have also analysed theoretically the effect of the addition of a second equivalent of **L1** on the energy barrier of the reductive elimination process, in order to probe whether the reaction is also under kinetic control. Consequently, two reaction pathways have been explored computationally, which differ in the nature of the initial products formed from reaction of [$PdMe_2$(tmeda)] with two equivalents of ligand **L1**, namely the two isomers: *penta*-coordinate

[$PdMe_2(\kappa^1$-P-**L1**$)(\kappa^2$-P,C-**L1**$)$] (**3**) (Scheme 5, Path B) having a square pyramidal geometry and *tetra*-coordinate square planar *cis*-[$PdMe_2(\kappa^1$-P-**L1**$)_2$] (**3'**) (L = **L1** in Scheme 5, Path C).

Computationally, the two complexes **3**[32] and **3'** are found to be *quasi*-isoenergetic (ΔG = 1.1 kcal mol^{-1}). Both **3** and **3'** are more stable than [$PdMe_2(\kappa^2$-P,C-**L1**$)$] (**1**) by 4.0 and 5.1 kcal mol^{-1}, respectively, something consistent with stabilisation of the Pd^{II} centre by the σ-donor ligands.[4] On probing the behaviour of **3** and **3'** computationally, the transition states for reductive elimination from each complex have been located (Fig. 1, paths B and C), and lie at $\Delta G^{‡}$ = 25.6 kcal mol^{-1} from **3'** ($\Delta G^{‡}$ = 20.5 kcal mol^{-1} from **1**) and 22.2 kcal mol^{-1} from **3** ($\Delta G^{‡}$ = 18.2 kcal mol^{-1} from **1**). Both these barriers to reductive elimination are significantly lower than that computed for the analogous process from **1**, *i.e.* with one equivalent of **L1** ($\Delta G^{‡}$ = 28.1 kcal mol^{-1}). Together, these computationally-derived results suggest that reductive elimination is more feasible from *penta*-coordinate complex **3**, than from its isomeric *tetra*-coordinate diphosphine analogue **3'**, consistent with earlier observations.[23]

The potential importance of the formation of *penta*-coordinate complexes in facilitating reductive elimination from *cis*-[$PdMe_2(\kappa^2$-P,C-**L1**$)$]-derived systems has been demonstrated experimentally and theoretically as described above. Indeed, it has been shown that reaction of [$PdMe_2$(tmeda)] with two equivalents of monodentate *aza*-norbornane ligand **L2**, rather than bidentate phosphine-alkene ligand **L1**, *cis*-[$PdMe_2(\kappa^1$-P-**L2**$)_2$] (**3'^{L2}**) is formed, which slowly (24 h, 0 °C) evolves into its *trans* isomer **3'^{L2}-*trans*** (Scheme 5, isomerization route, L = **L2**), without undergoing reductive elimination. Nevertheless, calculations predict a similar Gibbs energy barrier for reductive elimination from both the *tetra*-coordinate square planar Pd complexes **3'^{L2}** ($\Delta G^{‡}$ = 25.2 kcal mol^{-1})[33] and **3'^{L1}**, with the reaction being strongly exergonic in each case (from **3'^{L2}** ΔG = –31.2 kcal mol^{-1} and from **3'^{L1}** ΔG = –47.5 kcal mol^{-1}). From a computational standpoint, these data suggest that similar behaviour towards reductive elimination from both *cis*-[$PdMe_2(\kappa^1$-P-**L1**$)_2$] (**3'^{L1}**) and *cis*-[$PdMe_2(\kappa^1$-P-**L2**$)_2$]

(**3'**$^{\mathbf{L2}}$) complexes would be expected, contrary to what is observed experimentally. Consequently, the standard *tetra*-coordinate pathway for C–C reductive elimination from **3'** through $\mathbf{TS_{3',\rightarrow 2}}$ can be ruled out. Together, these latter results show that it is the formation of the *penta*-coordinate palladium intermediate **3**, which enhances the rate of reductive elimination from complex **1** when a second equivalent of phosphine-alkene ligand **L1** is added. Moreover, in combination with experimental observations, these computational analyses indicate that a significant role of the olefinic component of phosphine-alkene ligand **L1** is to act as a secondary tether site, with the resulting chelated complex being prevented from undergoing *cis-/trans*-isomerisation (as observed on treating [$PdMe_2$(tmeda)] with two equivalents of **L2**).

Thus, the combined computational and experimental studies described here give a potential explanation for the shorter reaction times observed experimentally for the formation of ethane from [$PdMe_2$(**L1**)$_n$] complexes where n=2 (*i.e.* a Pd:**L1** ratio of 1:2) compared with the situation where n=1 (Pd:**L1** = 1: 1). Thus, it is proposed that reductive elimination proceeds through the *penta*-coordinate intermediate **3** and the corresponding TS, $\mathbf{TS_{3\rightarrow 2}}$, which necessitates a ratio of Pd:**L1** = 1:2. Indeed, species **3** and $\mathbf{TS_{3\rightarrow 2}}$ are stabilised relative to [$PdMe_2$(κ^2-P,C-**L1**)] (**1**) and to its TS $\mathbf{TS_{1\rightarrow 2}}$, by ~5 and ~10 kcal mol^{-1}, respectively (Fig. 1). The greater stabilisation of the *penta*-coordinate transition state $\mathbf{TS_{3\rightarrow 2}}$ compared with that associated with **3** is consistent with a decrease in the reaction's activation barrier.

Using an approach developed by Korenaga et *al*. for a similar type of system,[34] direct information concerning the stabilisation of the $PdMe_2$ fragment, which results from coordination by **L1**, has also been obtained by computing the energies of the various fragments involved (Table 1). The structures of the reactants (**1**, **3'** and **3**) and the corresponding TS ($\mathbf{TS_{1\rightarrow 2}}$, $\mathbf{TS_{3',\rightarrow 2}}$ and $\mathbf{TS_{3\rightarrow 2}}$) were divided into phosphine fragments **L1** ([**L1**] or [**L1**]‡) and $PdMe_2$ fragments ([$PdMe_2$] or [$PdMe_2$]‡) and single point energy

calculations performed for each fragment in the same geometry as the original optimized complexes and transition states. The interaction energies in the reactants and in the TSs (ΔE_{int} and $\Delta E_{int}^{\ddagger}$) were then calculated as the energy difference between (**1**, **3** or **3'**)/corresponding **TS** and [**L1**]/[**L1**]‡ + $PdMe_2$/$PdMe_2^{\ddagger}$. When *penta*-coordinate (Table 1, Entries 1-2), the $PdMe_2$ fragment is highly stabilized (~21 kcal mol^{-1}), something that is even more apparent due to binding of **L1** in the transition state (~30 kcal mol^{-1}). Moreover, the stabilisation of the $PdMe_2$ fragment is augmented yet more when one of the **L1** ligands is chelating (Table 1, Entries 2-3). The stabilising effect of the alkene moiety is more important at the transition state (9.6 kcal mol^{-1}) than in the starting reactant (8.3 kcal mol^{-1}).

Table 1. Interaction binding energies (kcal mol^{-1}) relevant to the stabilisation of $PdMe_2$ by coordination of **L1**

Entry	Complex	ΔE_{int}	$\Delta E_{int}^{\ddagger}$	$\Delta\Delta E_{int} = \Delta E_{int} - \Delta E_{int}^{\ddagger}$
1	**1**	–64.3	–50.4	13.9
2	**3**	–85.0	–79.2	5.8
3	**3'**	–76.7	–69.6	7.1

To the best of our knowledge, the intermediacy of *penta*-coordinate species (and their corresponding transition states) in palladium-mediated $H_3C–CH_3$ coupling processes has been rarely considered.[23] Thus, it was of interest to probe both the structural features and electronic properties of **3** as well as those of the corresponding TS ($\mathbf{TS_{3\rightarrow 2}}$) in greater detail.

Following coordination of ligand **L1** to **1** to give *penta*-coordinate complex **3**, we compute that the P–Pd bond distance of the chelated κ^2-P,C-bound **L1** increases slightly (~0.04 Å). This is accompanied by a significant elongation of the Pd–CH_3 bond distances in

3, relative to those in complex **1**, with the increase in bond distance being greatest for the PdMe unit occupying a position *trans* to the olefinic moiety of the chelating **L1** (Fig. 2). Interestingly, these changes are paralleled by a slight reduction in the Me–Pd–Me bond angle from 86.2° (**1**) to 83.0° (**3**), which is in line with reductive elimination being more facile from complex **3**.[20]. In concert with the above changes, the C=C bond length of the palladium-bound olefinic moiety increases from 1.388 Å (**1**) to 1.420 Å (**3**), which is suggestive of an increase in back-donation from the Pd centre to the $\pi^*_{C=C}$ orbital (see below). The increase in the Pd–Me distances on going from complex **1** to complexes **3'** and **3** (Fig. 2) is corroborated by the respective bond strengths for each species obtained *via* AIM analysis. Summation of the electron density at both Pd–Me bond critical points (BCP), $\rho(\mathbf{r}_{BCP})_s$, indicates that the Pd–Me bonds are slightly stronger in **1** ($\rho(\mathbf{r}_{BCP})_s = 22\times10^{-2}$ au) than in either **3** (20×10^{-2} au) or **3'** (21×10^{-2} au). This is consistent with the larger computed $\Delta G^{\ddagger}$ values for the reductive elimination process (that results in the formation of ethane) from **1** compared to **3** or **3'**. A similar correlation between the energy barriers associated with reductive elimination and Pd–C bond strengths has been reported previously by Love and co-workers for cross-coupling reactions of polyfluoroarenes *via* C–F activation.[16c]

When the *penta*-coordinate intermediate complex **3** evolves to its transition state ($\mathbf{TS_{3\rightarrow2}}$), a slight change in geometry about the palladium centre occurs (Figs. 1 and 2). This results in a distorted square pyramidal structure in which the incoming ligand maintains the same position, while the Pd atom is displaced to slightly above the basal plane. This distortion was measured by defining the angle θ, which lies between the two planes defined by the fragments Me-Pd-Me and P-Pd-C_{olefin}, and increases from θ = 22.5° to 33.0°. As would be expected for the observed ethane-forming C–C coupling process, both Pd–Me distances are lengthened (2.33 Å in $\mathbf{TS_{3\rightarrow2}}$ *versus* 2.15 Å in **3**) and the Me–Pd–Me bond angle is reduced

(23.4%). It is also notable that the Pd–Me distances for $\mathbf{TS_{3\rightarrow 2}}$ are ~4 % longer than those of $\mathbf{TS_{1\rightarrow 2}}$ while the Me–Pd–Me bond angle is more acute in $\mathbf{TS_{3\rightarrow 2}}$ (51.6°) than in $\mathbf{TS_{1\rightarrow 2}}$ (55.5°).

On going from species **3'** to $\mathbf{TS_{3'\rightarrow 2}}$ (Fig. 2) the geometry around palladium changes from being slightly distorted square planar (θ'= 5.7°)[35] to distorted tetrahedral (θ' = 47.0°). The observed distortion in $\mathbf{TS_{3'\rightarrow 2}}$ is in agreement with what is commonly reported in the literature for $[PdMe_2(L)_2]$ complexes.[16a,36] Furthermore, for $\mathbf{TS_{3'\rightarrow 2}}$ the Pd–Me bond distances (2.13 and 2.23 Å) are similar to those of $\mathbf{TS_{3\rightarrow 2}}$ (average 2.24 Å), while the Me–Pd–Me bond angle is slightly wider (55.2° *versus* 54.3°). Together these data indicate that reductive elimination from complex **3'** requires a greater degree of structural rearrangement than is the case for reductive elimination from complex **3**, something that favours the reaction of the latter.

In summary, the theoretical studies undertaken here highlight the mutual relationship between the Gibbs energy barriers for reductive elimination for **1**, **3** and **3'** and the Pd–Me bond distances in these species preceding C–C bond formation. In addition, at the TS we observe that there is also a correlation between the values of $\Delta G^{\ddagger}$ and the Me–Pd–Me bond angles, as would be expected. Thus, longer/weaker Pd–Me bond distances/bonds and smaller Me–Pd–Me bond angles correlate with smaller barriers to reductive elimination.

Electronic properties of phosphine-alkene ligand L1

In order to gain a deeper understanding of the electronic impact of the phosphine-alkene ligand **L1** on alkyl-alkyl coupling reactions *via* reductive elimination from $PdMe_2$-containing systems, a study of the electron density at palladium was performed since it is now well-established that a metal's electron density has a significant influence upon the ease of reductive elimination.[5] Thus, we undertook a computational analysis of the charges associated with complexes **1**, **3** and **3'**, as well as for the corresponding transition states $\mathbf{TS_{1\rightarrow 2}}$, $\mathbf{TS_{3\rightarrow 2}}$

and $\mathbf{TS_{3'\rightarrow 2}}$, by means of NBO and AIM analyses. In particular, investigations of the differences in atomic charge at Pd, *q*(Pd), were made as a function of the mode of coordination of ligand **L1**, comparing chelating (κ^2-P,C) and monodentate (κ^1-P) binding in complexes **3** and **3'**, and as a function of the metal's coordination number (*tetra*-coordinate complex **1** *versus penta*-coordinate **3**).

Examination of the square planar complex **1** reveals that the *q*(Pd) parameter is significantly positive ($q(\mathrm{Pd})^{\mathrm{NBO}}$ = 0.33 au; $q(\mathrm{Pd})^{\mathrm{AIM}}$ = 0.27 au), despite the σ-donor effect of the bound phosphine moiety. Notably, for complex **1** a Natural Localized Molecular Orbital (NLMO) analysis indicates that there is a significant degree of electron density transferred from the Pd d orbitals to the bound olefin moiety of **L1**, consistent with the olefin's π-acceptor character (see ESI). This interaction is confirmed by the more positive charge at palladium, *q*(Pd), for **1** than for **1'**.[37]

The palladium centre of the intermediate complex **3'** ($q(\mathrm{Pd})^{\mathrm{NBO}}$ = 0.16 au; $q(\mathrm{Pd})^{\mathrm{AIM}}$ = 0.12 au) is less positively charged than the Pd in complex **1**, something consistent with the presence of two σ-donating Pd-bound phosphine ligands in **3'**. Surprisingly, in contrast, the palladium centre of the *penta*-coordinate *bis*(phosphine) complex **3** is only very slightly more positive ($q(\mathrm{Pd})^{\mathrm{NBO}}$ = 0.40 au; $q(\mathrm{Pd})^{\mathrm{AIM}}$ = 0.28 au) than the Pd atom in **1**, despite **3** bearing two σ-donating phosphine moieties. The similarity in the degree of positive charge associated with the palladium centres in complexes **1** and **3** is explained by the fact that in **3**, significant negative charge is associated with the olefinic carbons of the chelating **L1** ligand ($q(\mathrm{C_{olefin}})^{\mathrm{NBO}}$ = –0.33 au; $q(\mathrm{C_{olefin}})^{\mathrm{AIM}}$ = –0.08), which essentially neutralises the electronic impact of the additional σ-donating phosphine moiety. This effect is reflected by NLMO analysis in a slightly greater degree of back-donation from the palladium centre to the $\pi^*_{\mathrm{C1=C1'}}$ orbital in **3** compared to that determined for **1** (see ESI).

Taken together, NBO and AIM analyses show that on adding a second equivalent of ligand **L1** to complex **1** to form **3**, or on going from a *tetra*- to the *penta*-coordinate intermediate (**3'** *versus* **3**), leads to an increase in the positive charge at palladium. This is in good agreement with the lower barrier to elimination computed for complex **3** ($\Delta G^{\ddagger}$ = 22.2 kcal mol^{-1}) compared to either that determined for **1** ($\Delta G^{\ddagger}$ = 28.1 kcal mol^{-1}) or for **3'** ($\Delta G^{\ddagger}$ = 25.6 kcal mol^{-1}). Indeed, this trend is consistent with the fact that electron-poor metal centres will favour reductive elimination.[10,11] However, if the overall variation in the extent of positive charge localised on the palladium centres of the three complexes **1**, **3'** and **3** is analysed, there is no overall correlation between these values and those of $\Delta G^{\ddagger}$ for the reductive elimination reactions. Notably, a similar lack of correlation between either Mulliken or NPA charges at platinum and activation barriers was reported by Sakai and *al.* following an investigation of C(sp^2)–C(sp^2) coupling and subsequent elimination from *cis*-[PtPh$_2$(diphosphine)] complexes.[34]

In contrast, a good correlation between the computed values of *q*(Pd) determined for the palladium centres of the species identified at the corresponding transition states (**TS$_{1\rightarrow2}$**, **TS$_{3'\rightarrow2}$** and **TS$_{3\rightarrow2}$**) and Gibbs energy barriers to elimination is observed. Both NBO- and AIM-computed charges indicate that the value of *q*(Pd) becomes more positive (*i.e.* the electron density at palladium decreases) on going from **TS$_{1\rightarrow2}$** ($q(\mathrm{Pd})^{\mathrm{NBO}}$ = –0.03 au, $q(\mathrm{Pd})^{\mathrm{AIM}}$ = –0.05 au) to **TS$_{3'\rightarrow2}$** ($q(\mathrm{Pd})^{\mathrm{NBO}}$ = 0.08 au, $q(\mathrm{Pd})^{\mathrm{AIM}}$ = –0.04 au) and **TS$_{3\rightarrow2}$** ($q(\mathrm{Pd})^{\mathrm{NBO}}$ = 0.29 au, $q(\mathrm{Pd})^{\mathrm{AIM}}$ = 0.12 au). This trend is mirrored by the corresponding computed activation energy barriers (kcal mol^{-1}) for $H_3C–CH_3$ coupling, which decrease in the order **TS$_{1\rightarrow2}$** (28.1) > **TS$_{3'\rightarrow2}$** (25.2) > **TS$_{3\rightarrow2}$** (22.5). Thus, as the computed degree of positive charge at palladium increase, so the computed energy barrier to reductive elimination decreases, as anticipated.

Together, these observations concerning the charges associated with the various constituents of complexes **1**, **3** and **3'** and the associated transition states on the path to

reductive elimination are consistent with the electronic properties of the phosphine-alkene ligand **L1**. In particular, they reflect the electron-withdrawing character of the olefin moiety, which slightly increases its π-acceptance as reductive elimination progresses (back-donation from d_{xz}(Pd) to the $\pi^*_{C=C}$ increases by 3 kcal mol^{-1} from initial reactant to TS.

Influence of addition of auxiliary ligands (PPh_3, propene) on reductive elimination from 1

As previously described (computationally and experimentally), the addition of a second equivalent of **L1** to complex **1** forms a *penta*-coordinate species **3**, which undergoes reductive elimination with a rate considerably greater than that of complex **1** alone. Notably, a similar rate enhancement for reductive elimination from **1** can be achieved on addition of 5 mol% PPh_3. Here again it is proposed that the increase in rate results from the initial formation of a *penta*-coordinate species **4** (Scheme 5, Path B, L = PPh_3) on addition of phosphine to **1**. Although such a process is thermodynamically feasible (ΔG = –0.2 kcal mol^{-1}), it is slightly less favoured than for the formation of *penta*-coordinate complex **3** (ΔG = –4.0 kcal mol^{-1}) involving P-only ligation of **L1**. This difference can be attributed to the increased acceptor character of the amido-substituted phosphine component of **L1**, compared to that of PPh_3.[38] The TS, $\mathbf{TS_{4\rightarrow 2}}$, leading to the reductive elimination from the *penta*-coordinate complex [$PdMe_2$(κ^1-P–**PPh_3**)(κ^2-P,C-**L1**)] (**4**) is found at 22.5 kcal mol^{-1} (ESI Table S1), an energy difference very similar to that computed between **3** and its corresponding TS ($\Delta G^{\ddagger}$ = 22.2 kcal mol^{-1}), which is consistent with the similarity in the experimentally-determined rates of reductive elimination (5h for **1**+**L1** and 7 h for **1**+PPh_3). On considering the thermodynamics of the reductive elimination reaction, the process is about 2 kcal mol^{-1} more exergonic with ligand **L1** (**1**→**2** : –47.5 kcal mol^{-1}) than with PPh_3 (**1**→**4** : –45.1 kcal mol^{-1}). Since the more exergonic the coupling the faster the reaction, the small, but

significant differences in rate observed for reductive elimination from **3** and **4** (~ 2 h) are likely to be thermodynamic in origin (ESI: influence of PPh_3 on reductive elimination).

It has also been demonstrated experimentally that an increase in the rate of reductive elimination from complex **1** may be achieved through addition of 5 mol% propene. This agrees well with the recent observation that the barrier to reductive elimination from *cis*-[$PdMe_2(PPh_3)_2$] may be lowered significantly on addition of an electron-withdrawing olefin to forming *cis*-[$PdMe_2$(olefin)(PPh_3)].[14] In contrast to what has been computed for the addition of phosphine ligands (**L1** or PPh_3) to complex **1**, the formation of the *penta*-coordinate species [$PdMe_2(\eta^2\text{-}C_2H_4)(\kappa^2\text{-P,C-}$**L1**)] (**5**) is thermodynamically unfeasible (ΔG = 11 kcal mol^{-1}) (Scheme 5, Path B, L = propene).[39] This suggests that on addition of propene to [$PdMe_2(\kappa^2$-P,C-**L1**)] (**1**), the subsequently-observed C–C coupling and reductive elimination reactions proceed through the direct TS (**$TS_{1\rightarrow 2}$**) rather than from the *penta*-coordinate intermediate **5**. Thus, the decrease in the reaction time for reductive elimination from **1** in the presence of propene (5 mol%), 30 h *versus* 120 h, is believed to result exclusively from the stabilization of the intermediate low coordinate complex [$Pd(\kappa^2$-P,C-**L1**)] (**2'**), which reacts with propene to form initially [$Pd(\kappa^2$-P,C-**L1**)(propene)] (**2''**) (Scheme 5, Path B, Table S2 ESI) that then rapidly evolves to afford complex **2**. More details are given in ESI.

Experimental data and computational studies involving elimination reactions from the PdCl(Me) fragment

Since we have demonstrated, both experimentally and computationally, that the potentially-chelating phosphine-alkene ligand **L1** significantly enhances the rates of $C(sp^3)$–$C(sp^3)$ coupling *via* reductive elimination from Pd^{II} complexes, it was of interest to explore the potential of this metal scaffold to promote more challenging reductive elimination

processes. To this end, we have undertaken a combined experimental/computational investigation of alkyl–halide coupling reactions involving ligand **L1**. Due to significant M–Cl bond polarisation, the barrier to alkyl-chloride reductive elimination is much greater than that for alkyl–alkyl eliminations. Consequently, to the best of our knowledge no examples of this type of coupling process involving Pd^{II} have been reported.[40]

Experimental results

Addition of **L1** to *cis*-[PdCl(Me)(cod)] (Pd : **L1** = 1 : 1) does indeed give rise to Pd^0 complex **2** in an extremely rapid reaction in which complete consumption of **L1** is achieved within seconds at –40 °C, but which is accompanied by the formation of an equimolar quantity of the methyl phosphonium chloride salt of ligand **L1**, **8**, and leaves unreacted palladium(II) starting material.[22] In contrast, treating *cis*-[PdCl(Me)(cod)] with three equivalents of **L1** both rapidly and quantitatively affords a 1 : 1 mixture of Pd^0 complex **2** and methyl phosphonium salt **8** as the only products (Scheme 6). Although the formation of complex **2** can be regarded as indicative of a reductive elimination process having taken place, the formation of **8** is indicative of an alternative reaction pathway. Despite repeated attempts, the extremely rapid rates of reaction of **L1** with *cis*-[PdCl(Me)(cod)] and subsequent coupling/elimination processes precluded detailed spectroscopic and mechanistic investigation; consequently, a computational study was launched.

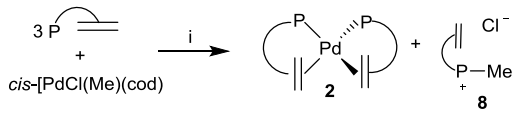

Scheme 6 (i) toluene, r.t., > 99%.

Reaction profile for *pseudo*-reductive elimination from PdCl(Me)

Since both the palladium(0) complex **2** and methyl phosphonium chloride **8** are formed in equimolar quantities, as a starting point for this investigation we initially considered a direct reaction sequence, which may be regarded as Me-Cl coupling followed by reaction between ligand **L1** and the chloromethane (Scheme 7). Thus, we have explored computationally pathways (Gibbs free energy profiles) leading to the direct formation of MeCl *via* reductive elimination from the square planar complex *cis*-[PdCl(Me)(κ^2-P,C-**L1**)] (**6**) (Scheme 7, Path A) and from the square pyramidal *penta*-coordinate complex [PdCl(Me)(κ^1-P-**L1**)(κ^2-P,C-**L1**)] (**7**) (Scheme 7, Path B). Pathways A and B are entirely analogous to those explored earlier for CH_3/CH_3 coupling and reductive elimination *via* complexes **1** and **3** (*vide supra*).

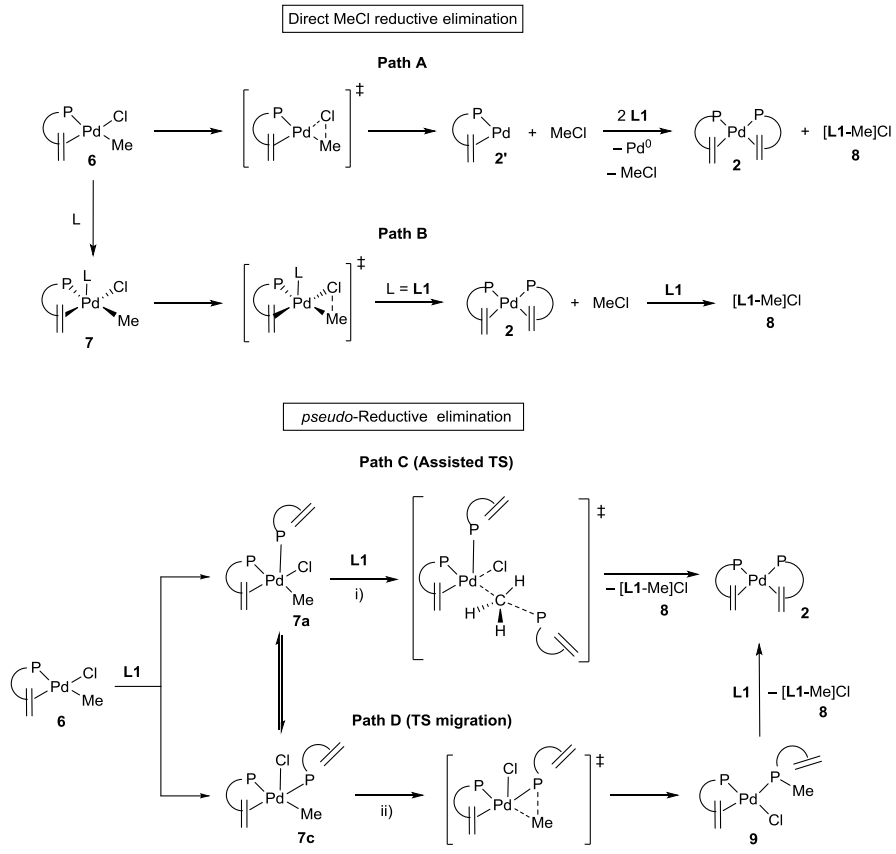

Scheme 7 Possible reaction pathways for the formation of palladium(0) complex **2** and methyl phosphonium salt **8** from *cis*-[PdCl(Me)(κ^2-P,C-**L1**)] (**6**) and *penta*-coordinate [PdCl(Me)(κ^1-P-**L1**)(κ^2-P,C-**L1**)] (**7**).

Formation of MeCl *via* direct reductive elimination from complex **6**[41] is clearly unfeasible, with a Gibbs energy barrier of ~43 kcal mol^{-1} being computed.[42] However, a direct reductive elimination pathway from *penta*-coordinate complex **7** is slightly more energetically accessible, with a value of $\Delta G^{\ddagger}$ of ~38.0 kcal mol^{-1} (see below) being determined. Nevertheless, it remains very high and, as a result, the formation of **2** and **8** from [PdCl(Me)(cod)] cannot proceed through this type of pathway.

It should be noted that for completeness, barriers to elimination were computed for each of the three energetically accessible isomers (**a**-**c**) of the square-pyramidal species **7** found on the potential energy surface and topologically connected by Berry *pseudo*-rotations, (See ESI, Fig. S4), each of which is computed to be more stable than their parent complex **6**.[43] Two isomers place the Cl ligand in the square coordination plane, located either *trans* to the phosphorus (**7a**) or *trans* to the olefin moiety (**7b**). The energy difference between these two isomers is ~6 kcal mol^{-1}, with isomer **7a** being the lower in energy. The third isomer **7c**, in which the Cl ligand is located above the square plane, is essentially isoenergetic with **7a** (ΔG = 1.4 kcal mol^{-1}). Consequently, taking these data together, only isomers **7a** and **7c** have been probed computationally.

A comparison of the energies of the *penta*-coordinate complexes **7a,c** shows that they are stabilized by approximately 12 kcal mol^{-1} relative to the parent *tetra*-coordinate complex and **L1**. Notably, this stabilization of the *penta*-coordinate complexes is slightly greater than that for the corresponding complex [PdMe$_2$(κ^1-P-**L1**)(κ^2-P,C-**L1**)] (**3**) involved in CH_3-CH_3 coupling (12 *versus* 4.0 kcal mol^{-1}). The transition states (T**S**$_{\mathbf{7\rightarrow 2}}$) for Me–Cl coupling *via* reductive elimination lie 38 kcal mol^{-1} (Fig. 3) above their *penta*-coordinate precursors, **7**.[44] Despite both the chelating nature of **L1** and its potential to act as a π-acceptor through coordination of its olefinic component, the barriers determined for direct elimination from complexes **6** and **7** are entirely comparable to those computed for a range of *cis*-

[PdCl(Me)(PR_3)$_2$] complexes involving both strongly and weakly Lewis basic *mono*-dentate phosphine ligands.[17] Furthermore, the barriers for the formation of MeCl from complexes **6** and **7** are 16 ~ kcal mol^{-1} higher than those computed for the formation of ethane through Me/Me coupling *via* a direct mechanism from, respectively, *cis*-[PdMe$_2$(κ^2-P,C-**L1**)] (**1**) and [PdMe$_2$(κ^1-P-**L1**)(κ^2-P,C-**L1**)] (**3**), as expected.[4,14] The greater stabilization of the *penta*-coordinate intermediate **7** *versus* **3** (–12.5 kcal mol^{-1} and –4 kcal mol^{-1}, respectively) in relation to the *tetra*-coordinate complexes **6** and **1**, respectively, as well as the destabilization of the *penta*-coordinate transition state $\mathbf{TS_{7\rightarrow 2}}$ *versus* $\mathbf{TS_{3\rightarrow 2}}$, is consistent with the 16 kcal mol^{-1} greater activation barrier for the reductive elimination of Me–Cl compared to that for Me–Me. Moreover, formation of MeCl from **7a**, is computed to be less thermodynamically favourable than from **6** (ΔG : +3.0 kcal mol^{-1} from **7a**; ΔG : -9.3 kcal mol^{-1} from **6**). The energy penalty associated with the formation of MeCl *via* this type of direct process is in stark contrast to that for the formation of ethane through Me/Me coupling from **3** (ΔG : –47.1 kcal mol^{-1} from **3**).

Thus, it is evident that even if the *penta*-coordinate complexes **7** are formed from **6**, not only is the activation barrier to a direct reductive elimination process leading to the formation of MeCl very high, but the reaction is only weakly exergonic, making this overall transformation both kinetically unfeasible and only weakly thermodynamically favoured. As a result, such a *direct* reaction pathway is inconsistent with the rapid rate of reaction observed experimentally on treating *cis*-[PdCl(Me)(cod)] with two or three equivalents of **L1**.

Consequently, an alternative *pseudo*-reductive elimination mechanism that accounts for the experimental observation that three equivalents of **L1** are needed to complete the reaction of *cis*-[PdCl(Me)(cod)] was sought.[22] To this end, two reaction pathways involving *penta*-coordinate species **7** have been examined : a ligand-assisted pathway involving a

bimolecular TS in which the phosphorus lone pair of the incoming ligand **L1** attacks the palladium-bonded methyl group (Scheme 7, Path C); and a palladium-to-phosphorus methyl migration (Scheme 7, Path D).

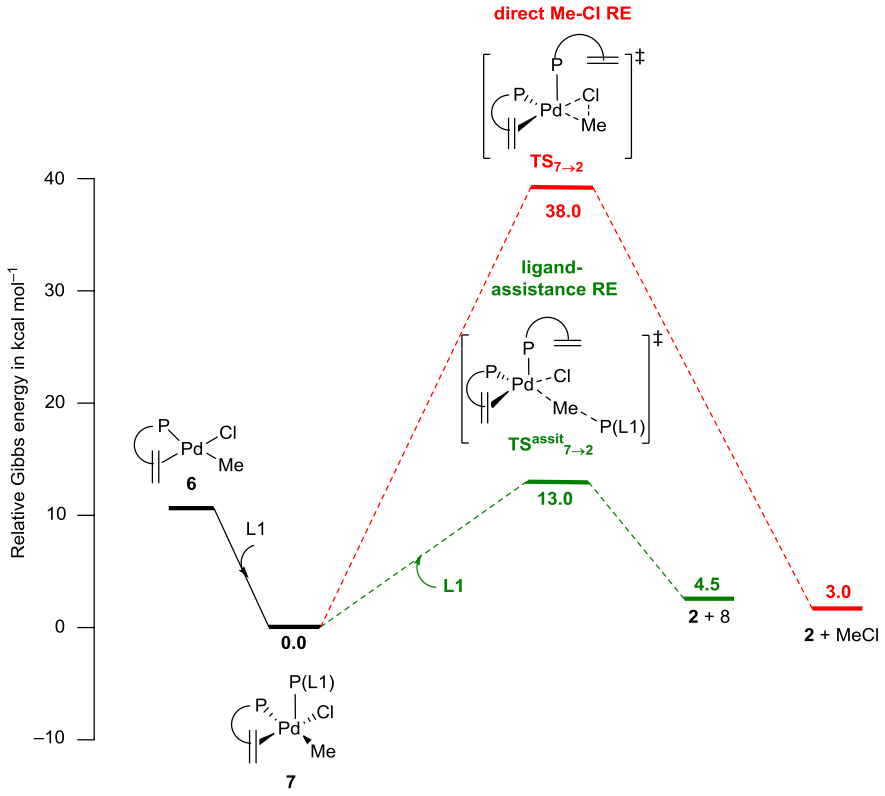

Fig. 3 Gibbs free energy profile (ΔG values in kcal mol^{-1}) for the direct MeCl reductive elimination (RE) (in red) from *penta*-coordinate intermediate [Pd(Me)Cl(κ^1-P-**L1**)(κ^2-P,C-**L1**)]. Ligand-assisted pathway (in green) for MeCl reductive elimination affording complex **2** and the phosphonium salt **8**.

A comparison of the two proposed reaction mechanisms reveals that the computed TS (**TS**$^{\textbf{assist}}_{\textbf{7→2}}$) for the ligand-assisted pathway (Fig. 3, Gibbs free energy profile), $\Delta G^{\ddagger}$ = 13.0 kcal mol^{-1},[45] is lower in energy, than that computed for the TS in the palladium-to-phosphorus methyl migration pathway ($\Delta G^{\ddagger}$ = 28.9 kcal mol^{-1}; ESI Fig. S5). Since the intermediate **9** (Scheme 7, Path D), formed after the methyl migration, is thermodynamically unfavourable

(ΔG = 25.8 kcal mol^{-1}; reversible reaction) and the activation barrier is higher than that for the assisted ligand path, the palladium-to-phosphorus methyl migration pathway has been discarded. For the ligand-assisted pathway the low activation barrier is in good agreement with the rapid reaction observed experimentally.

For this ligand-assisted reaction manifold, the mechanism is concerted (a single step from **7**. Thus, simultaneous formation of an (**L1**)P···Me and rupture of a Me···Pd bond occurs. This process proceeds through a TS that strongly resembles that of an S_N2-like reaction in which the phosphorus donor component of **L1** attacks the palladium-bound methyl ligand. Indeed, this type of S_N2-like reaction between a metal-bound methyl ligand and a tertiary phosphine was proposed by Weinberg and Baird in order to account for the formation of the phosphonium salt [Ph_3PMe]Cl from [$RhCl_2(Me)(CO)(PPh_3)_2$].[46] In our case, the similarity between the TS for the ligand-assisted elimination reaction pathway with that involved in a classical S_N2-type process is further reinforced by the computed Pd···Me···P(**L1**) bond angle of 165.0° and by the identification of a planar *pseudo-penta*-coordinate carbon, which is located approximately equidistant from both the Pd and P atoms (Pd–C and C–P distances of 2.49 and 2.35 Å, respectively). The identity of this species as the true transition state is confirmed on following the intrinsic reaction coordinate (IRC). In the forward direction, the IRC gives rise to the two experimentally-observed products, complex **2** and the methyl phosphonium chloride salt **8**, while moving in the reverse direction the TS is connected to the starting reactants, **7a** and **L1**.

As mentioned above, it is reasonable to suggest that the *penta*-coordinate complexes **7** are formed *in situ* through reaction of **L1** with *cis*-[PdCl(Me)(cod)] *via* formation of the square planar complex **6**. A comparison of the computed structures of complexes **6** and **7** reveals that on addition of **L1**, an elongation, and hence weakening of both the Pd–Cl (**6**: 2.09 Å; **7**: 2.13 Å) and Pd–Me (**6**: 2.37 Å; **7**: 2.56 Å) bonds is determined, and is accompanied by a

slight narrowing of the Me–Pd–Cl bond angle from 89.6° to 87.9°. The change in bond strength is evidenced from the sum of the values of the electron density, $\rho(\mathbf{r})$, at each BCP ($\rho_s(\mathbf{r})$ = 19×10^{-2} au in **6** and 16×10^{-2} au in **7**). Together these structural changes are consistent with the notion that reductive elimination from *penta*-coordinate complex **7** is easier than from **6** ($\Delta G^{\ddagger}$ ~ 43 kcal mol^{-1}from **6** and $\Delta G^{\ddagger}$ ~ 38 kcal mol^{-1} from **7**).

Examination of the MOs involved in the reaction of **L1** with the palladium-bound methyl ligand of **7a** further supports the analogy between this process and a classical S_N2-like reaction (Fig. 4). In particular, the LUMO of **TS$^{assist}_{7\rightarrow2}$** corresponds to an antibonding combination of the phosphorus lone pair (n_P) of the incoming ligand **L1** and the σ^*_{PdC} orbital of complex **7a** (see Fig. S7, ESI). The HOMO of **TS$^{assist}_{7\rightarrow2}$** is mainly composed of the d_z^2 orbital of palladium and the phosphorus lone pair of the incoming ligand **L1** (with a minor contribution from the 2pπ^* orbital of the carbon of the methyl group).

The reaction pathway involving the proposed S_N2-like process is also supported by the relevant Bader charges. Summation of the atomic charges, $\sum q(\Omega)$, in the incoming phosphine-alkene ligand **L1** at the assisted TS (**TS$^{assist}_{7\rightarrow2}$**), reveals a formal positive charge (+0.32 au) in agreement with its nucleophilic character. Furthermore, the phosphorus atom of the incoming third equivalent of **L1** has lost 0.32 electrons, resulting in an atomic charge at P in the **TS$^{assist}_{7\rightarrow2}$** of +1.95 au compared with +1.63 au for the free ligand, consistent with complete charge transfer from incoming **L1** to complex **7** *via* the phosphorus atom. This electron density is transferred mainly to the palladium centre, whose atomic positive charge decreases on going from **7** (+0.35 au) to the **TS$^{assist}_{7\rightarrow2}$** (+0.21 au), while the charge at the C_{methyl} atom remains essentially constant.

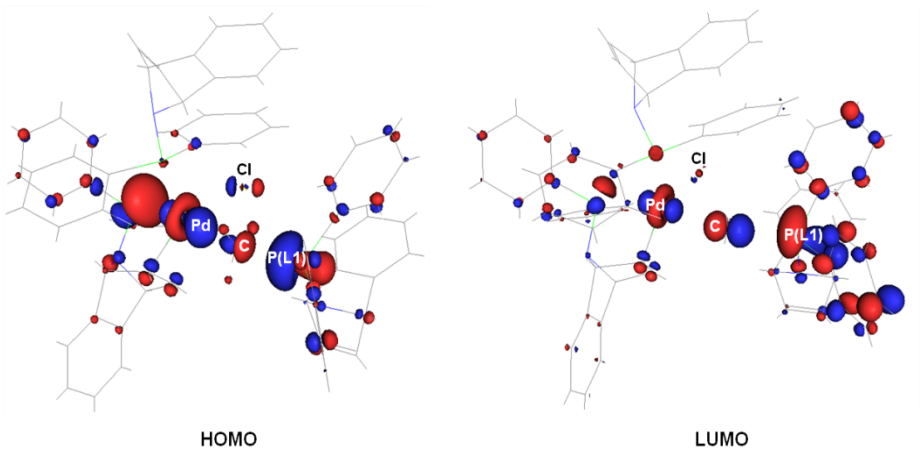

Fig. 4 Frontier Molecular Orbitals for $TS^{assist}_{7\rightarrow 2}$ involved in the assisted pathway (Scheme 7, Path C, assisted TS).

Relative to the barriers determined for direct reductive elimination from complexes **6** or **7**, the Gibbs energy barrier for the ligand-assisted elimination process, resulting from addition of a further equivalent of **L1** to *penta*-coordinate intermediate **7**, is found to be 25 kcal mol^{-1} lower, which is in good agreement with the experimentally-observed reaction rates.[22] The ligand-assisted pathway involves a *pseudo*-reductive elimination through an S_N2-like transition state in which the palladium-bound methyl group is slightly activated towards nucleophilic attack by the incoming phosphine **L1**, with a slight stabilisation of the acceptor σ^*_{Pd-C} orbital being computed on going from **6** (–1.8 eV) to **7** (–1.9 eV). Furthermore, this mechanism is favoured as a result of the stability of the leaving group, namely the *bis*(phosphine-alkene)Pd^0 complex **2**. Thus, overall, the combination of all of the comparatively small, but still significant structural and electronic changes associated with the reaction of **6** with excess ligand **L1**, together with the formation of the stable phosphonium salt **8** and stable Pd^0 complex **2**, render this *pseudo*-reductive elimination reaction both

kinetically and thermodynamically favourable. Nevertheless, the very low activation barrier, suggests that this mechanism is largely under kinetic control.

Conclusion

The use of a joint experimental-theoretical approach in probing reductive elimination processes involving palladium(II) systems has confirmed the importance of phosphine-alkene ligand **L1** in facilitating C(sp^3)-C(sp^3) and indirect C(sp^3)-Cl coupling processes. The presence of both ligand σ-donor and π-acceptor sites allows chelation, prevents isomerization processes and permits access to a *penta*-coordinate intermediate [$PdMe_2$(κ^1-P-**L**)(κ^2-P,C-**L1**)] (L = phosphine-alkene ligand **L1**, PPh_3) from [$PdMe_2$(κ^2-P,C-**L1**)] (**1**) after addition of donor ligand L. This *penta*-coordinate intermediate undergoes facile reductive elimination and plays a key role in the mechanisms for these elimination reactions. A decrease in the activation barrier of $\Delta G^{\ddagger}$ ~6 kcal mol^{-1} from the chelated square planar complex *cis*-[$PdMe_2$(κ^2-P,C-**L1**)] (**1**) to *penta*-coordinate [$PdMe_2$(κ^1-P-**L1**)(κ^2-P,C-**L1**)] (**3**) is observed and is consistent with a significant stabilisation of the *penta*-coordinate transition state $\mathbf{TS_{3\rightarrow 2}}$. Moreover, a very stable palladium(0) *bis*(phosphine-alkene) complex [Pd(κ^2-P,C-**L1**)$_2$] (**2**) is formed in a strongly exergonic reaction, which makes the C–C coupling process irreversible. The activation barriers and the reaction rates for the reductive elimination can both be correlated with the variation of the main structural features of the corresponding transition state (Me–Pd distance and Me–Pd–Me bond angle) and the electron density at the metal centre (more electron-poor Pd centre). It has been demonstrated, both experimentally and computationally, that addition of PPh_3 to **1** affords [$PdMe_2$(PPh_3)(κ^2-P,C-**L1**)], which behaves in an analogous fashion to the corresponding complex bearing two **L1** ligands, facilitating reductive elimination (quasi-similar activation barrier and strongly exergonic reactions). Together, the

experimental and theoretical data suggest that reductive elimination promoted by chelating phosphine–alkene ligand **L1** is, albeit indirectly, both kinetically and thermodynamically controlled. Nevertheless, thermodynamic factors are a key parameter in determining the rates of elimination.

Direct Me–Cl coupling *via* reductive elimination from the *penta*-coordinate [PdCl(Me)(κ^1-P-**L1**)(κ^2-P,C-**L1**)] complex has been computed to be highly unfeasible as would be anticipated as a consequence of the strong, significantly ionic Pd–Cl bond. However, in the presence of three equivalents of the phosphine-alkene ligand **L1**, *cis*-[PdCl(Me)(cod)] undergoes a rapid indirect reductive elimination process, which affords the methyl phosphonium chloride salt of **L1** and the Pd^0 complex **2**. It has been shown computationally, that this reaction proceeds through a bimolecular S_N2-like TS, in which the phosphorus lone pair of the incoming third equivalent of ligand **L1** attacks the palladium-bonded methyl group, in a process with an energy barrier $\Delta G^{\ddagger}$ ~25 kcal mol^{-1} lower than that for direct Me–Cl elimination. Thus, the use of the phosphine-alkene ligand **L1** significantly facilitates what can be described as an extremely rare *pseudo*-reductive elimination of MeCl. The chelating nature of **L1** enhances the formation of the *penta*-coordinate intermediate **7**, which is strongly stabilized, with the *penta*-coordination promoting this ligand-assisted elimination mechanism. In contrast with the direct $C(sp)^3$–$C(sp)^3$ coupling, this ligand makes this *pseudo*-reductive elimination of MeCl feasible due to kinetic control.

Computational details

Calculations were carried out using density functional theory (DFT) in the Kohn−Sham formulation as implemented in Gaussian 09,[47] to locate *minima* and transition states on the potential energy surface of the systems studied. The B97-D functional was

used.[48] Palladium atom was described with the SDD[49] (electron core potential (ecp-60-mwb)) pseudo-potential and associated basis set, augmented by a set of f-orbital polarization functions.[50] The 6-31G** basis set[51] was employed for all other atoms. All stationary points involved were fully optimized, without any symmetry restrictions. Frequency calculations were undertaken to confirm the nature of the stationary points, yielding one imaginary frequency for transition states (TS), corresponding to the expected process, and zero for *minima*. The connectivity of the transition states and their adjacent minima was confirmed by intrinsic reaction coordinate (IRC) calculations.[52] Zero-point energy (ZPE) corrections were carried out for all computed energies. Gibbs free energies were calculated by using the harmonic approximation and standard textbook procedures. All thermodynamic and structural parameters mentioned in the text refer to the reaction paths optimized in the gas phase at 298 K.

Atoms in Molecules (AIM) theory[53] and Natural Bond Orbital (NBO)[54] theory have been used to compute the electron atomic charges using AIMAll code[55] and the NBO-5 program, respectively.[56] The former was also employed to carry out the topological analysis [$\rho(\mathbf{r})$] on selected structures, while the latter was also used to quantify the effect of the π-acceptor character of the alkene ligand in these Pd complexes.

Molecular orbitals were drawn with Molekel.[57]

Acknowledgements

The Centre National de la Recherche Scientifique, the Université de Pau et des Pays de l'Adour, Durham University (including a scholarship to L. Tuxworth), and the EPSRC are warmly acknowledged for financial support of this work. The theoretical work was granted access to the HPC resources of IDRIS under allocation 2013 (i2013080045) made by GENCI

(Grand Equipement National de Calcul Intensif). The MCIA (Mesocentre de Calcul Intensif Aquitain) is also thanked for providing calculation facilities. L. Estevez thanks the Xunta de Galicia for the postdoctoral contract under the I2C program. The "Agence Nationale de la Recherche" (ANR-10-BLAN-070901) is also gratefully acknowledged for contribution to the financial support of the L. Estevez. Johnson Matthey is acknowledged for the loan of palladium salts.

Supporting Information Available

Electronic supplementary information (ESI) available: theoretical results and cartesian coordinates for the optimized structures and their transition states.

Notes and references

[a] *Institut des Sciences Analytiques et de Physico-Chimie pour l'Environnement et les Matériaux (IPREM). Université de Pau et des Pays de l'Adour/CNRS UMR 5254, Hélioparc, 2 Avenue du Président Angot, 64053 Pau cedex 09, France. E-mail : karinne.miqueu@univ-pau.fr, Fax : + 33 (0) 559 407 862; Tel + 33 (0) 559 407 577.*

[b] *Departamento de Química Física, Universidade de Vigo, Facultade de Química Lagoas-Marcosende s/n, 36310 Vigo, Galicia, Spain.*

[c] *Centre for Sustainable Chemical Processes, Department of Chemistry, Durham University, South Road, Durham, DH1 3LE, UK. E-mail : p.w.dyer@durham.ac.uk, Fax : + 44 (0) 191 334 2150 ; Tel : + 44 (0) 191 384 4737.*

[d] *Department of Chemistry, Durham University, South Road, Durham, DH1 3LE, UK.*

1 J. Tsuji, *Palladium Reagents and Catalysts: New Perspectives for the 21st Century*, John Wiley & Sons Publishers, Chichester, 2nd edn, 2004.
2 J. F. Hartwig, *Acc. Chem. Res.*, 1998, **31**, 852.
3 E. Negishi, *Handbook of organopalladium Chemistry for Organic Synthesis*, John Wiley & Sons Publishers, New York, 2002.
4 L. Xue and Z. Lin, *Chem. Soc. Rev.*, 2010, **39**, 1692.
5 J. F. Hartwig, *Inorg. Chem.*, 2007, **46**, 1936.
6 J. M. Brown and N. A. Cooley, *Chem. Rev.*, 1988, **88**, 1031.
7 *(a)* J. F. Hartwig, M. Kawatsura, S. I. Huack, K. H. Shaughnessy and L. M. Alcaraz-Roman, *J. Org. Chem.*, 1999, **64**, 5575; *(b)* A. F. Littke and G. C. Fu, *Angew. Chem. Int. Ed.*, 2002, **41**, 4176; *(c)* U. Christmann and R. Vilar, *Angew. Chem. Int. Ed.*, 2005, **44**, 366.
8 *(a)* E. Negishi, T. Takahashi and K. Akiyoshi, *J. Organomet. Chem.*, 1987, **334**, 181; *(b)* M. Yamashita, J. V. C. Vicario and J. F. Hartwig, *J. Am. Chem. Soc.*, 2003, **125**, 16347; *(c)* L. Abis, A. Sen and J. Halpern, *J. Am. Chem. Soc.*, 1978, **100**, 2915.
9 A. Dedieu, *Chem. Rev.*, 2000, **100**, 543.
10 K. Tatsumi, R. Hoffmann, A. Yamamoto and J. K. Stille, *Bull. Chem. Soc. Jpn.*, 1981, **54**, 1857.
11 *(a)* J. J. Low and W. A. Goddard III, *J. Am. Chem. Soc.*, 1986, **108**, 6115; *(b)* J. J. Low and W. A. Goddard III, *Organometallics*, 1986, **5**, 609.
12 V. P. Ananikov, D. G. Musaev and K. Morokuma, *Eur. J. Inorg. Chem.*, 2007, 5390.
13 A. Ariafad and B. F. Yates, *J. Organomet. Chem.*, 2009, **694**, 2075.
14 M. Pérez-Rodrígez, A. A. C. Braga, M. Garcia-Melchor, M. H. Pérez-Temprano, J. A. Casares, G. Ujaque, A. R. de Lera, R. Álvarez, F. Maseras and P. Espinet, *J. Am. Chem. Soc*., 2009, **131**, 3650.
15 V. P. Ananikov, D. G. Musaev and K. Morokuma, *Organometallics*, 2005, **24**, 715.
16 *(a)* S. A. Macgregor, G. W. Neave and C. Smith, *Faraday Discuss.*, 2003, **124**, 111; *(b)* E. Zuidema, P. W. N. N. van Leeuwen and C. Bo, *Organometallics*, 2005, **24**, 3703; *(c)* A. D. Sun and J. A. Love, *Dalton Trans.*, 2010, **39**, 10362.
17 P. K. Sajith and C. H. Suresh, *Inorg. Chem.*, 2011, **50**, 8085.
18 *(a)* J. Hartwig, *Nature*, 2008, **455**, 314; *(b)* J. F. Hartwig. *Angew. Chem. Int. Ed. Engl.*, 1998, **37**, 2046; *(c)* Catalyzed Carbon-Heteroatom Bond Formation, Wiley 2011, Weinheim, A. K. Yukin, Ed.
19 *(a)* J. P. Wolfe, S. Wagaw, J. F. Marcoux, and S. L. Buchwald, *Acc. Chem. Res.*, 1998, **31**, 805; *(b)* C. Amatore and A. Jutand, *Acc. Chem. Res.*, 2000, **33**, 314; *(c)* M. Beller, T. H. Riermeier in J.

Mulzer, H. Waldmann (Eds.), *Organic Synthesis Highlights*, VCH, **1998**; *(d)* T. Hiyama, E. Shirakawa in *Handbook of Organopalladium Chemistry for Organic Synthesis*, Vol. 1 (Eds.: E. Negishi, A. de Meijere), Wiley, New York, 2002, pp. 285 – 309
20 J. E. Marcone and K. G. Moloy, *J. Am. Chem. Soc.*, 1998, **120**, 8527.
21 *(a)* E. Gioria, J. M. Martínez-Ilarduya, D. García-Cuadrado, J. A. Miguel, M. Genov and Pablo Espinet, *Organometallics*, 2013, **32**, 4255; *(b)* H. Zhang, X. Luo, K. Wongkhan, H. Duan, Q. Li, L. Zhu, J. Wang, A. S. Batsanov, J. A. K. Howard, T. B. Marder and A. Lei, *Chem. Eur. J.*, **2009**, 15, 3823.
22 L. W. Tuxworth, L. Baiget, A. Phanopoulos, O. J. Metters, A. S. Batsanov, M. A. Fox, J. A. K. Howard and P. W. Dyer, *Chem. Comm*, 2012, **48**, 10413.
23 K. Tatsumi, A. Nakamura, S. Komiya, A. Yamamoto and T. Yamamoto, *J. Am. Chem. Soc.*, 1984, **106**, 8181.
24 R. H. Crabtree, *The Organometallic Chemistry of the Transition Metals*, Wiley, Hoboken, 5th edn, 2009.
25 J. Forniés, A. Martín, L. F.Martín and B. Menjón, *Organometallics*, 2005, **24**, 3539.
26 A. G. Orpen and N. G. Connelly, *J. Chem. Soc., Chem. Commun.*, 1985, 1310.
27 *(a)* M. Brookhart and M. L. H. Green, *Organomet. Chem.*, 1983, **250**, 395; *(b)* D. Braga, F. Grepioni, E. Tedesco, K. Biradha and G. R. Desiraju, *Organometallics*, 1997, **16**, 1846; *(c)* M Brookhart, M. L. H. Green and G. Parkin, *Proceedings of the National Academy of Sciences*, 2007, **104**, 6908.
28 R. F. W. Bader *J. Chem. Phys. A*, 1998, **102**, 7314.
29 J. P. Stambuli, C. D. Incarvito, M. Buhl and J. F. Hartwig, *J. Am. Chem. Soc.*, 2004, **126**, 1184.
30 Note, the *tri*-coordinate olefin complex [$PdMe_2(\kappa^1$-C-κ^2-C_{olefin}-**L1**)] could not be located on the PES. Instead, this structure rearranges to give the isomer [$PdMe_2(\kappa^2$-C_{olefin},N-**L1**)] in which **L1** is bound in a chelating fashion with an η^2-alkene and the N atom bound to Pd. The energy difference between this isomer and the model *tri*-coordinate T-shaped complex *cis*-[$PdMe_2(\kappa^1$-P-**L1**)] **1'** is negligible and the activation barrier for reductive elimination from this complex is calculated to be 20.3 kcal mol^{-1}, slightly higher than that from **1'** (15.8 kcal mol^{-1}).
31 M. Garcia-Melchor, A. A. C. Braga, A. Lledos, G. Ujaque and F. Maseras, *Accounts of Chem. Res.*, 2013, **46**, 2626.
32 The square pyramidal geometry, where one of the methyl group is an apical position is higher in energy by 14.4 kcal mol^{-1}.
33 The *cis*/*trans*-isomerisation process (Scheme 5, Path C) is more feasible than reductive elimination from **3'**. For the privileged dissociative mechanism, the limiting step of the reaction is ligand dissociation (20 kcal mol^{-1}) to form a 14 e^- T-shaped intermediate. The barrier for dissociation is lower than that for reductive elimination. The intermediate then rearranges *via* a Y-shaped TS to give another T-shaped intermediate (7.7 kcal mol^{-1}) from which the *trans* square planar complex is formed by association of a ligand (a barrier-less process). Isomerisation can also occur *via* a tetrahedral TS with an activation barrier that is also calculated to be ~20 kcal mol^{-1} lower in energy that that for reductive elimination. Although it is established that *cis*-/*trans*-isomerisation for Pd^{II} systems can proceed *via* an associative pathway, this has not been considered here since only two equivalents of **L2** are available and coordination of the reaction solvent (CH_2Cl_2) is not expected.
34 T. Korenaga, K. Abe, A. Ko, R. Maenishi and T. Sakai, *Organometallics*, 2010, **29**, 4025.
35 θ' is the dihedral angle between the two planes defined by the P-Pd-P and Me-Pd-Me units.
36 S. Sakaki, N. Mizoe, Y. Musashi, B. Biswas and M. Sugimoto, *J. Phys. Chem. A*, 1998, **102**, 8027.
37 In complex **1'** the palladium charge q(Pd) is +0.20 au (NBO) or 0.14 (AIM).
38 P. W. Dyer, J. Fawcett, M. J. Hanton, R. D. W. Kemmitt, R. Padda and N. Singh, *Dalton Trans.*, 2003, 104.
39 With other functionals such as B3PW91 or M06 the *penta*-coordinate Pd complex with propene does not exist on the potential energy surface, while both DFT methods agree with B97D for the other calculations relating to the complexes where L = **L1** or PPh_3.
40 *(a)* A. Vigalok and A. W. Kaspi, *Top. Organomet. Chem.*, 2010, **31**, 19; *(b)* P. K. Sajith and C. H. Suresh, *Inorg. Chem.*, 2011, **50**, 8085.

41 Two isomers **6a** and **6b** can be envisaged, one with Cl *cis* to P (**6a**) and the other with Cl *trans* to the olefin (**6b**). The energy difference between this two isomers is negligible, 1 kcal mol^{-1} using the B97D functional.
42 From **6a**, $\Delta G^{\ddagger}$ = 42.6 kcal mol^{-1} and from **6b**, $\Delta G^{\ddagger}$ = 43.7 kcal mol^{-1}.
43 The *penta*-coordinate [PdCl(Me)(κ^1-P-**L1**)(κ^2-P,C-**L1**)] complex with Me in apical position is 23.6 kcal mol^{-1} higher in energy than complex **7a** (Fig. S4 in ESI).
44 From **7a**, **7b** and **7c**, the transition states for Me–Cl coupling *via* reductive elimination are located at, respectively, 38.0, 37.2 and 38.4 kcal mol^{-1}.
45 The activation barrier from complex **6** for the ligand-assisted pathway involving a bimolecular TS in which the phosphorus lone pair of the incoming ligand **L1** attacks the methyl group, is calculated to be higher in energy at 29.4 kcal mol^{-1} (Fig. S5 in ESI).
46 E.L. Weinberg and M. C. Baird, *Journal of Organometallic Chemistry*, 1979, **179**, C61.
47 *Gaussian 09. Revision **C.01*** M. J. Frisch, G. W. Trucks, H. B. Schlegel, G. E. Scuseria, M. A. Robb, J. R. Cheeseman, G. Scalmani, V. Barone, B. Mennucci, G. A. Petersson, H. Nakatsuji, M. Caricato, X. Li, H. P. Hratchian, A. F. Izmaylov, J. Bloino, G. Zheng, J. L. Sonnenberg, M. Hada,. M. Ehara, K. Toyota, R. Fukuda, J. Hasegawa, M. Ishida, T. Nakajima, Y. Honda, O. Kitao, H. Nakai, T. Vreven, J. A. Montgomery, Jr. J. E. Peralta, F. Ogliaro, M. Bearpark,J. J. Heyd, E. Brothers, K. N. Kudin, V. N. Staroverov, R. Kobayashi, J. Normand, K. Raghavachari, A. Rendell, J. C. Burant, S. S. Iyengar, J. Tomasi, M. Cossi, N. Rega, J. M. Millam, M. Klene, J. E. Knox, J. B. Cross, V. Bakken, C. Adamo. J, Jaramillo, R. Gomperts, R. E. Stratmann, O. Yazyev, A. J. Austin, R. Cammi, C. Pomelli, J. W. Ochterski, R. L. Martin, K. Morokuma, V. G. Zakrzewski, G. A. Voth, P. Salvador, J. J. Dannenberg, S. Dapprich, A. D. Daniels, Ö. Farkas, J. B. Foresman, J. V. Ortiz, J. Cioslowski and D. J. Fox. Gaussian. Inc. Wallingford CT. 2009.
48 S. Grimme, *J. Comp. Chem.*, 2006, **27**, 1787.
49 *(a)* B. Metz, H. Stoll and M. Dolg, *J. Chem. Phys.*, 2000, **113**, 2563; *(b)* M. Dolg, *Modern Methods and Algorithm of Quantum Chemistry*, *Vol. 1*, Ed.: J. Grotendorst, John von Neuman Institute for Computing, Jülich Germany, 2000,479–508; *(c)* D. Andrae, U. Haeussermann, M. Dolg, H. Stoll and H. Preuss, *Theor. Chim. Acta.*, 1990, **77**, 123; *(d)* M. Dolg, U. Wedig, H. Stoll and H. Preuss, *J. Chem. Phys.*, 1987, **86**, 866.
50 A. W. Ehlers, M. Böhme, S. Dapprich, A. Gobbi, A. Höllwarth, V. Jonas, K. F. Köhler, R. Stegmann, A. Veldkamp and G. Frenking, *Chem. Phys. Lett.*, 1993, **208**, 111.
51 P. C. Hariharan and J. A. Pople, *Theor. Chim. Acta*, 1973, **28**, 213.
52 *(a)* C. Gonzalez and H. B. Schlegel. *J. Chem. Phys.*, 1989, **90**, 2154; *(b)* C. Gonzalez and H. B. Schlegel, *J. Phys. Chem.*, 1990, **94**, 5523.
53 *(a)* R. F. W. Bader, *Atoms in Molecules - A Quantum Theory*, Oxford University Press: Oxford, 1990; *(b)* R. F. W. Bader, *Chem. Rev.*, 1991, **91**, 893; *(c)* C. F. Matta and R. J. Boyd, *The Quantum Theory of Atoms in Molecules - From Solid State to DNA and Drug Design*, Ed.: Weinheim, Wiley-WCH, 2007.
54 *(a)* E. Reed, L. A. Curtiss and F. Weinhold, *Chem. Rev*., 1988, **88**, 899; *(b)* J. P. Foster and F. Weinhold, *J. Am. Chem. Soc.*, 1980, **102**, 7211; *(c)* A. E. Reed and F. Weinhold, *J. Chem. Phys.*, 1985, **83**, 1736.
55 AIMAll (Version 11.12.19), T. A. Keith, TK Gristmill Software, Overland Park KS, USA, 2011 (aim.tkgristmill.com).
56 NBO 5.0. E. D. Glendening, J, K. Badenhoop, A. E. Reed, J. E. Carpenter, J. A. Bohmann, C. M. Morales and F. Weinhold, Theoretical Chemistry Institute, University of Wisconsin, Madison, 2001.
57 *Ugo Varetto, MOLEKEL 5.6, Swiss National Supercomputing Centre: Lugano (Switzerland).*